NAVAL POSTGRADUATE SCHOOL
Monterey, California

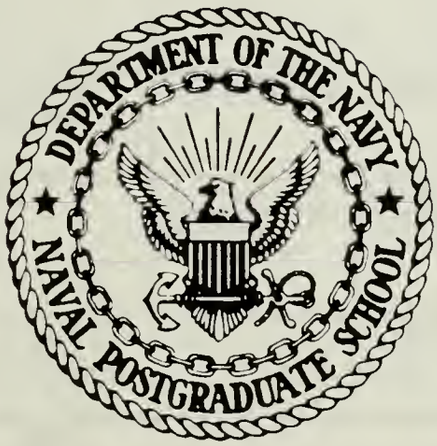

THESIS

AN EXPERIMENTAL TEST OF MINORITY CARRIER ANNEALING ON GALLIUM ARSENIDE SOLAR CELLS USING FORWARD-BIASED CURRENT

by

Thomas Fredrick Clark

September 1986

Thesis Advisor: Sherif Michael

SECURITY CLASSIFICATION OF THIS PAGE

REPORT DOCUMENTATION PAGE

1a REPORT SECURITY CLASSIFICATION UNCLASSIFIED	1b. RESTRICTIVE MARKINGS
2a SECURITY CLASSIFICATION AUTHORITY	3 DISTRIBUTION / AVAILABILITY OF REPORT Approved for public release; distribution unlimited
2b DECLASSIFICATION / DOWNGRADING SCHEDULE	
4 PERFORMING ORGANIZATION REPORT NUMBER(S)	5 MONITORING ORGANIZATION REPORT NUMBER(S)
6a. NAME OF PERFORMING ORGANIZATION Naval Postgraduate School 6b OFFICE SYMBOL (If applicable) 62	7a. NAME OF MONITORING ORGANIZATION Naval Postgraduate School
6c. ADDRESS (City, State, and ZIP Code) Monterey, California 93943-5000	7b. ADDRESS (City, State, and ZIP Code) Monterey, California 93943-5000
8a NAME OF FUNDING / SPONSORING ORGANIZATION 8b. OFFICE SYMBOL (If applicable)	9. PROCUREMENT INSTRUMENT IDENTIFICATION NUMBER
8c. ADDRESS (City, State, and ZIP Code)	10 SOURCE OF FUNDING NUMBERS PROGRAM ELEMENT NO / PROJECT NO / TASK NO / WORK UNIT ACCESSION NO

11 TITLE (Include Security Classification) AN EXPERIMENTAL TEST OF MINORITY CARRIER ANNEALING ON GALLIUM ARSENIDE SOLAR CELLS USING FORWARD-BIASED CURRENT

12 PERSONAL AUTHOR(S)
Thomas Fredrick Clark

13a TYPE OF REPORT	13b TIME COVERED	14 DATE OF REPORT (Year, Month, Day)	15 PAGE COUNT
Master's Thesis	FROM _____ TO _____	1986 September 26	86

16 SUPPLEMENTARY NOTATION

17 COSATI CODES			18 SUBJECT TERMS (Continue on reverse if necessary and identify by block number)
FIELD	GROUP	SUB-GROUP	Gallium Arsenide; Solar Cells; Annealing

19 ABSTRACT (Continue on reverse if necessary and identify by block number)

There has been recent interest in providing an on-orbit solar cell annealing capability. Minority carrier injection annealing was examined using a 0.5A/cm^2 forward-biased current density on gallium arsenide solar cells in a 90 degree centigrade ambient environment. The cells had been irradiated with 1-Mev electrons for a total fluence of 3E15el/cm^2. When annealing stopped, after 48 hours, the procedure had recovered 30% of the maximum power that was lost due to radiation damage. This procedure may have on-orbit potential.

20 DISTRIBUTION / AVAILABILITY OF ABSTRACT	21 ABSTRACT SECURITY CLASSIFICATION
☐ UNCLASSIFIED/UNLIMITED ☒ SAME AS RPT ☐ DTIC USERS	UNCLASSIFIED
22a NAME OF RESPONSIBLE INDIVIDUAL Prof Sherif Michael	22b TELEPHONE (Include Area Code) (408)646-2252 22c OFFICE SYMBOL 62Xp

DD FORM 1473, 84 MAR 83 APR edition may be used until exhausted
All other editions are obsolete

SECURITY CLASSIFICATION OF THIS PAGE

Approved for public release; distribution unlimited

An Experimental Test of Minority Carrier Annealing on Gallium Arsenide Solar Cells using Forward-biased Current

by

Thomas Fredrick Clark
Lieutenant, United States Navy
B.S., University of Oklahoma, 1979

Submitted in partial fulfillment of the
requirements for the degree of

MASTER OF SCIENCE IN ELECTRICAL ENGINEERING

from the

NAVAL POSTGRADUATE SCHOOL
September 1986

ABSTRACT

There has been recent interest in providing an on-orbit solar cell annealing capability. Minority carrier injection annealing was examined using a 0.5A/cm^2 forward-biased current density on gallium arsenide solar cells in a 90 degree centigrade ambient environment. The cells had been irradiated with 1-Mev electrons for a total fluence of 3E15e1/cm^2. When annealing stopped, after 48 hours, the procedure had recovered 30% of the maximum power that was lost due to radiation damage. This procedure may have on-orbit potential.

TABLE OF CONTENTS

LIST OF TABLES

LIST OF FIGURES

ACKNOWLEDGEMENT

The author wishes to thank Professor Sherif Michael for his guidance in the preparation of this thesis. Additionally, the author wishes to thank Peter Iles of Applied Solar Energy Corporation for providing the gallium arsenide solar cells used in the main experiment. A special thanks to my wife Barbara, who accepted the sound of a printer in the wee hours of the morning.

I. INTRODUCTION

Gallium arsenide solar cells are about to become the primary alternative to using silicon solar cells on Earth orbiting satellites. Silicon's advantages include low cost, ease of handling, light weight and good thermal capacitance. Gallium arsenide loses in each of the above catagories. It does have one redeeming quality, the gallium arsenide semiconductor is much more radiation tolerant than silicon.

There are two life limiting factors in today's Earth satellites. One is the amount of fuel carried on board for station keeping and other required maneuvers. The second is the lifetime of the electrical power generating system. In solar cell/battery power systems, the solar cell is the weak link.

Gallium arsenide allows the satellite designer to extend the power system life but with a substantial weight increase. If an increase in weight is not possible, then the total number of gallium arsenide solar cells must be reduced. Pound for pound the satellite lifetime will still be longer using a GaAs system although the cost per kilowatt or cost per year would be very high. A possible solution would be to anneal the solar cells while in-orbit. This would extend the life of a smaller and less expensive solar array.

Thermal annealing has been well known for years. A rather recent annealing technique is known as minority carrier injection. High current is passed in the cell from an external power supply or from an intense light source. There is mild interest today in Forward-bias Current Annealing. This process could be integrated into a satellite's electrical system and extend the solar cells' useful life, and therefore the satellite's lifetime. The literature does not address possible gains obtainable using this method. To use this process solar cell array designers will require data providing the expected recovery of a cell as a function of the radiation fluence, cell temperature, and the annealing current density.

This thesis will look at this process while imposing on it some of the limitations that exist on the satellite in the space environment.

In Chapter II a discussion of the radiation effects on solar cells will be found along with two measurement techniques that are very useful but difficult to implement. The space radiation environment is also addressed.

Chapter III defines the electrical parameters to be measured and the equipments used to do so.

Semiconductor and solar cell annealing is addressed in Chapter IV. The few papers that have carried the Forward-bias Current Annealing procedure into solar cells are discussed. These papers address the physical properties

of the annealing but do not extend to possible engineering applications.

The actual Forward-bias Current Annealing experiment is discussed in Chapter V. Calculation of the annealing rate can be found here. Several related experiments that were conducted can be found in Appendices A through C.

Finally, Chapter VI, Conclusions and Recommendations, discusses the implications of this process, possible errors in the test procedure and several follow-on experiments that should be conducted.

II. RADIATION EFFECTS ON SOLAR CELLS

A. RADIATION INTERACTIONS

When one speaks of the radiation effects on solar cells, one means the physical changes that occur in the device that result in electrical parameter degradation.

In the space environment, we are mainly interested in the high energy massive particle radiations such as electrons, protons, neutrons and ions. The fact that these particles may have charge, have mass and a wide energy range implies that more than one interaction may result. The primary interactions follow [Ref. 1: Chap. 3].

1. Inelastic Collisions with Atomic Electrons

This is the dominate mechanism by which 1 Mev electrons lose energy in an absorber and is an important process for proton energy loss. The absorber's electrons are moved to a higher energy state or are removed totally.

2. Elastic Collisions with Atomic Nuclei

The energetic charged particles may interact with the positive atomic nucleus through Rutherford scattering. The energy transferred to the atom may displace it from its lattice site. This energetic atom may inturn displace one or more other atoms. This is an important energy loss process for protons and it contributes somewhat to electron energy loss.

3. Inelastic Collisions with Atomic Nuclei

A high energy particle is absorbed by the atomic nucleus leaving it in an excited state. This nucleus then decays, ejecting energetic nucleons and recoiling through the lattice structure. The moving nucleus can itself cause additional dislocations. This nuclear activation and radioactive decay process has a very low probability of occurrence, but once initiated, it can add unwanted impurities to the crystalline lattice depending upon the decay process followed. This process is sometimes referred to as spallation.

B. TEMPORARY RADIATION DAMAGE

As can be seen from the above interactions, there are two types of radiation damage, ionization and atomic displacement. Ionization causes darkening of coverglass and adhesives as well as changing adhesive mechanical properties. This is of interest to the solar cell array designer but does not effect the cell directly. In the semiconductor material of the solar cell, ionization produces hole-electron pairs very much like that generated by visible light photons although roughly three times the energy is required for the same number of charge pairs. Therefore, the damage caused by ionization is only temporary in nature and is a desirable interaction.

Figures 1 and 2 are plots of the expected range and stopping power of silicon for electrons and protons. For range determination, the left axis values in the figures must be divided by 2.33 gm/cm^3, which is the density of the cell material. At 1-Mev, an electron will travel 0.39cm, or through the cell, while a proton will only travel 0.0017cm, 0.7mils, and will be absorbed in the coverglass if they are installed on the cells.

Yeh, et al [Ref. 2], have derived the empirical formulae in Table I for range and reduced energy for electrons and protons in GaAs. The 1-Mev electron travels 0.11cm and the proton travels 0.001cm in GaAs. Again, a coverglass would absorb low energy protons.

C. Permanent Radiation Damage

Permanent damage to crystalline absorbers results from atomic displacement due to high energy particles. There is a minimum displacement energy, E_d, for this damage to take place. For GaAs the energy is 25eV [Ref. 3] while E_d for Si is 12.9eV [Ref. 1, page 3.7]. The maximum energy that can be transferred from the energetic particle to the lattice atom is [Ref. 4]:

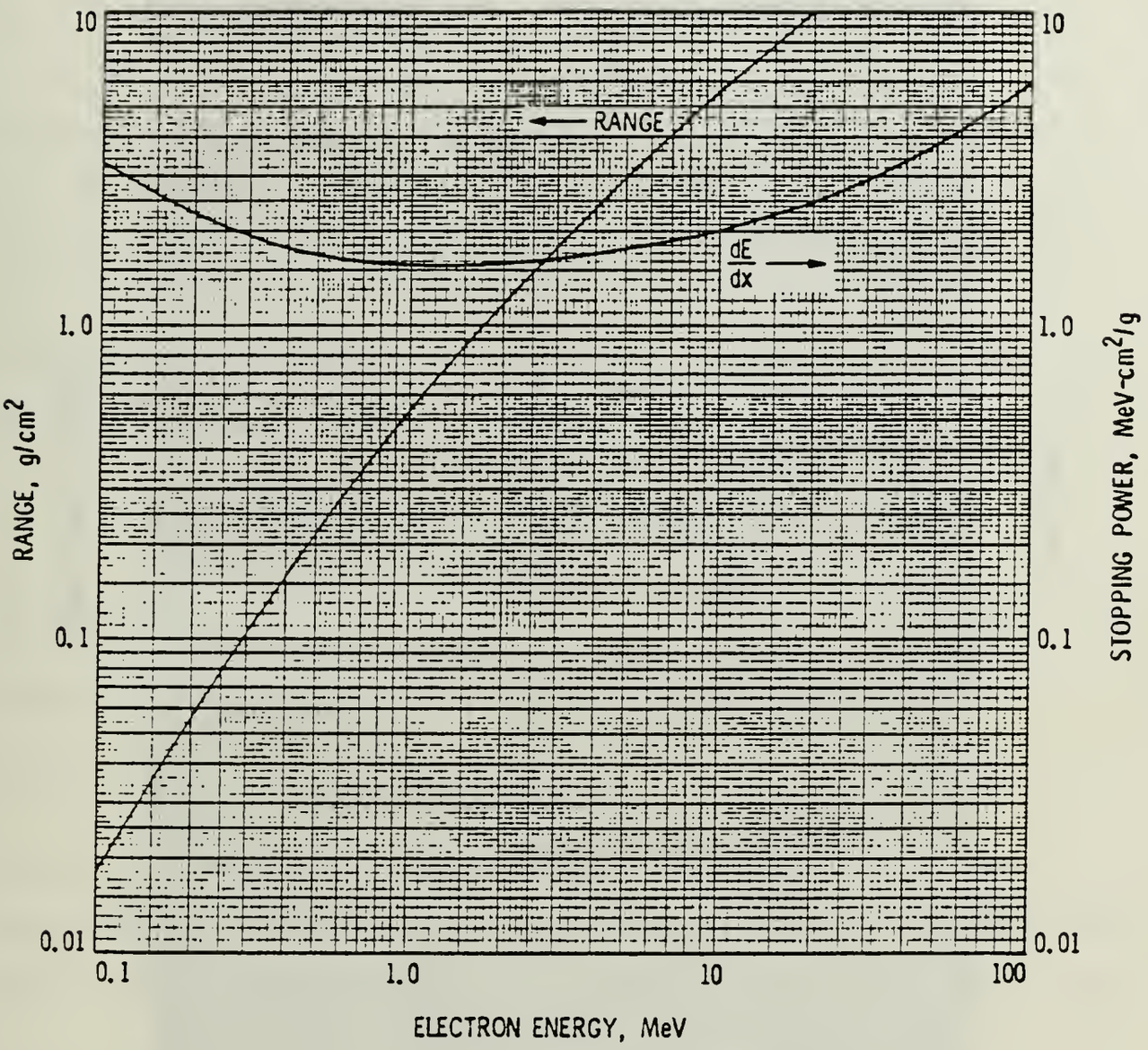

Figure 1 Stopping Power and Range Curves for Electrons in Silicon. [Ref. 1]

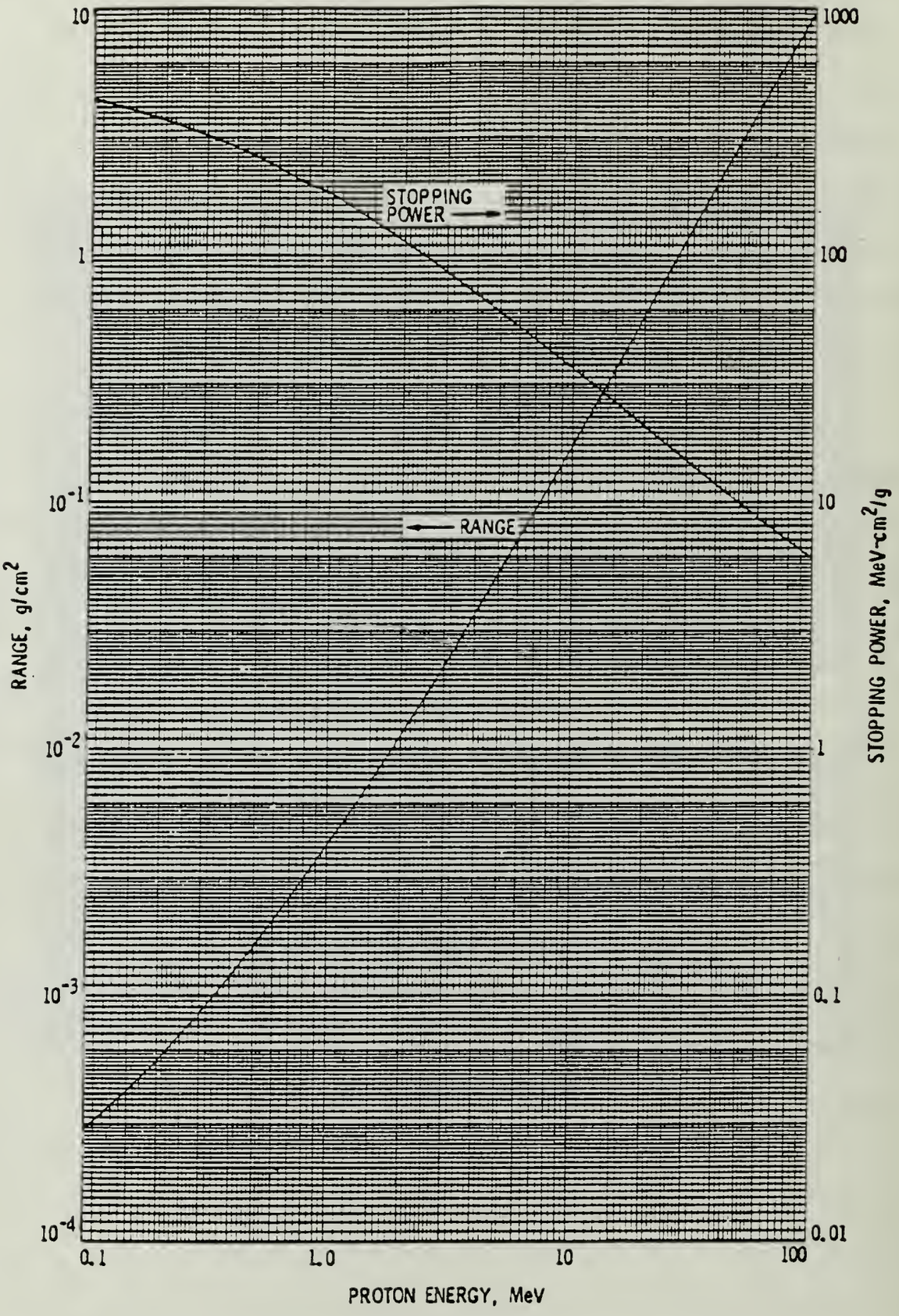

Figure 2 Stopping Power and Range Curves for Protons in Silicon. [Ref. 1]

TABLE I

EMPIRICAL FORMULAE OF RANGE AND REDUCED ENERGY FOR ELECTRONS AND PROTONS IN GaAs [Ref. 2]

ELECTRON

$R=-0.8763+100.042x+3528.8x^2-4997.51x^3$ $x<=0.2Mev$ (1)

$R=-48.067+700.994x+794.971x^2-341.5x^3$ $x<=1.0Mev$ (2)

$R=-250.77+1397.2x-39.4954x^2+0.82267x^3$ $x<=10.0Mev$ (3)

$E_{re}=1.061E-2+37.9136x-5465.826x^2+3.78864x^3$ $E_o<=0.1Mev$ (4)

$E_{re}=8.9865E-2+8.2195x-0.6236x^2+1.6267x^3$ $E_o<=10.0Mev$ (5)

PROTON

$R=0.00688+8.9414x-37.5326x^2+171.2658x^3$ $x<=0.1Mev$ (6)

$R=-0.00382+6.6356x+3.7874x^2-0.093355x^3$ $x<=5.0Mev$ (7)

$R=451.244-192.1x+32.1036x^2-1.3938x^3$ $x<=10.0Mev$ (8)

$E_{re}=-2.72E-4+9.69E-2x+1.284E-1x^2-8.97E-2x^3$ $E_o<=0.1Mev$ (9)

$E_{re}=1.05E-2+1.367E-1x-4.58E-3x^2+9.14E-5x^3$ $E_o<=1.75Mev$ (10)

$E_{re}=6.508E-1+5.2471E-2x-1.518E-4x^2+2.3E-7x^3$ $E_o<=10Mev$ (11)

where the particle range, R, is in micrometers,um;
the reduced energy, E_{re}, is in Mev;
and the thickness, x, used in the reduced energy equations are in micrometers, um.

$$E_{max} = 4*E_j*M1*M2/(M1+M2)^2 \quad \text{;for protons} \quad (12)$$

$$E_{max} = 2*E_j(E_j+2*m*c^2)/M2*c^2 \quad \text{;for electrons} \quad (13)$$

where E_{max} = maximum energy transferred

E_j = incident particle energy in eV

M1, M2 = the respective masses of particle and lattice atom

m = electron mass

c = velocity of light

Although non-coulombic collisions of neutrons with lattice atoms is unlikely, a single 1-Mev neutron can displaced 1500 Si atoms, clustering the damage around the initial reaction site. As seen from Table II, proton displacement collisions are very much more probable than similar electron collisions while the neutron interaction is the rarest. If $E_{max}>=E_d$ then the atom can be displaced to form stable defects. The number of displacements per unit volume, N_d, is:

$$N_d = n_a * @ * V * Theta \quad (14)$$

where n_a = atom density of the absorber

@ = displacement cross section(cm^2)

V = average displacements per primary displacement

Theta = radiation fluence(particles/cm^3)

Table III and Figure 3 give the defect number probabilities for GaAs where V is the number of recoils and P_v is the probability that V or more defects will result.

TABLE II

DISPLACEMENT CROSS SECTION(@) FOR SILICON [Ref. 1]

Particle Energy (Mev)	@ electron 10E-24	@ proton 10E-20	@ neutron 10E-24
1	68	3.5	2.4
2	73	1.8	
5	77	0.7	
10	77	0.35	
20	77	0.18	
40	77	0.09	

TABLE III

DEFECT PROBABILITIES FOR PROTONS AND ELECTRONS in GaAs [Ref. 5]

	Proton, E_p(MeV)				Electron, E_e(MeV)		
ν	.02	.05	.1	1	1	5	10
2	0.496	0.498	0.499	0.500	0.314	0.489	0.501
3	.243	.247	.249	.250	.046	.232	.249
4	.159	.164	.165	.167	.001	.145	.164
5	.117	.122	.123	.125	-	.103	.122
7	.075	.080	.082	.083	-	.060	.079
10	.047	.052	.054	.055	-	.033	.050

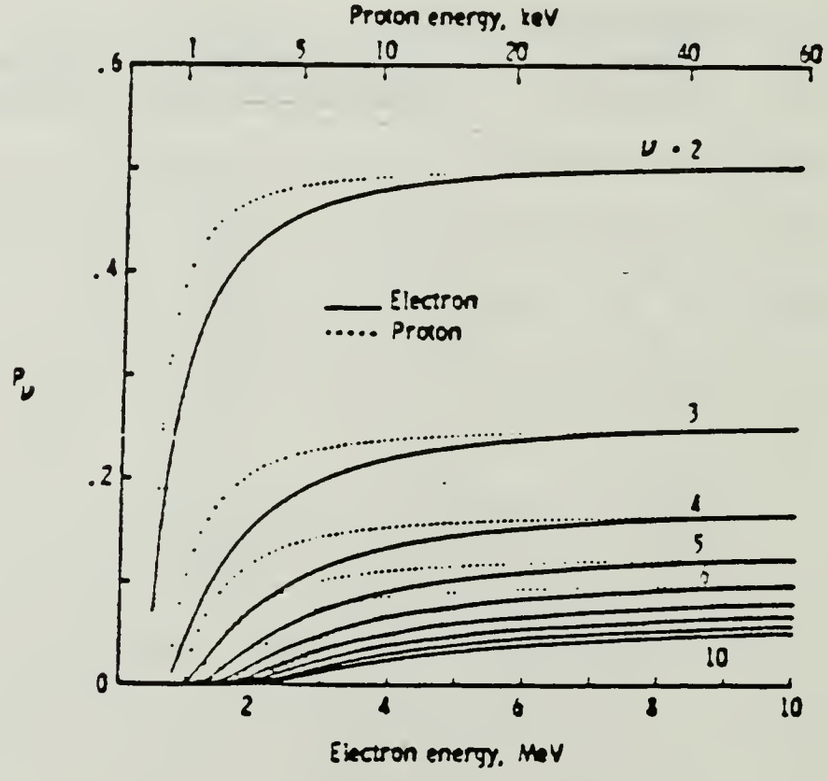

Figure 3 Defect Number Probabilities in GaAs [Ref. 5]

D. DEEP LEVEL TRANSIENT SPECTROSCOPY

There are several recent papers [Refs. 4,6,7] addressing Deep Level Transient Spectroscopy (DLTS) as a technique for investigating lattice displacement damage in GaAs caused by radiation. This technique observes the capacitive transients due to hole and electron traps that result from inconsistencies in the semiconductor crystalline lattice. Incomplete bonds, displaced atoms and other lattice defects cause recombination centers, traps, within the bandgap of the semiconductor material. Figure 4 shows a typical DLTS spectrum for GaAs that has been irradiated with 1-Mev electrons at a fluence of 1E15e1/cm^2.

Although each peak indicates a quantity of defects has occurred, no correlation can currently be made as to the exact nature of the defects. There does appear to be correlation with respect to the relative magnitudes of each peak and the total numbers of defects in the semiconductor as the result of radiation damage.

DLTS measurements are cumbersome, equipment intensive, and time consuming, but they have been useful in annealing studies by allowing the experimenter to actually observe, quantitatively, a decrease in lattice defects.

E. MINORITY CARRIER LIFETIME

With the exception of very low energy protons which causes displacement damage in the junction space charge

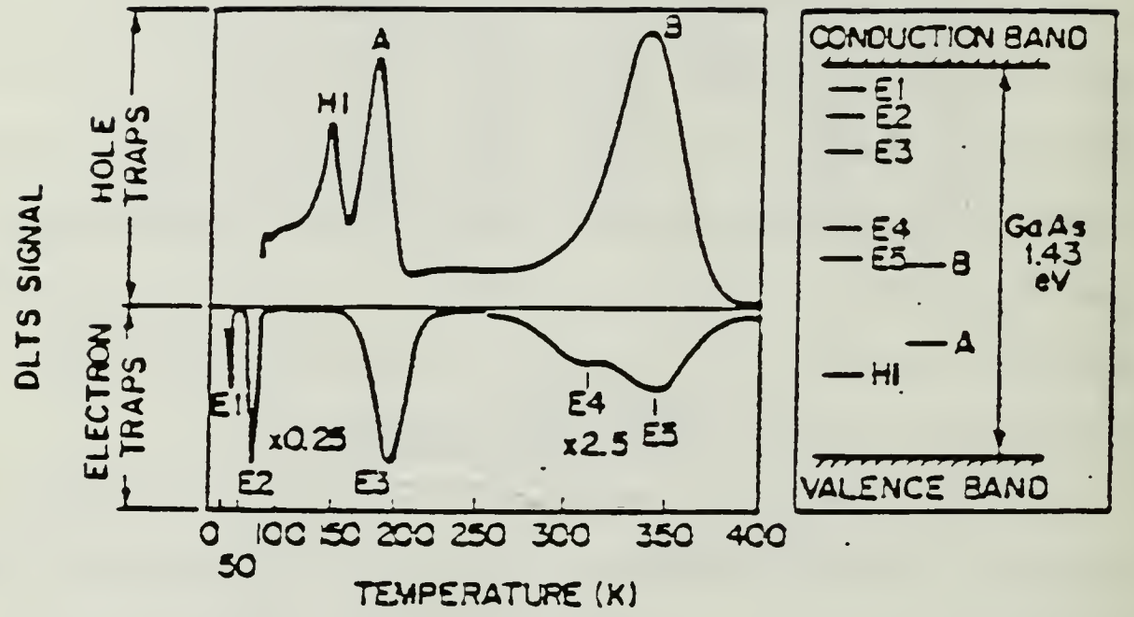

Fig. 4 DLTS spectrum of 1-MeV room-temperature electron-irradiated LPE n-GaAs. Positive DLTS peaks ($H1$, A, B) are due to hole traps (in n-type material), while negative peaks ($E1,\ldots,E5$) are due to electron traps. The A and B hole traps are present in as-grown LPE GaAs; the other six levels are introduced by 1-MeV-electron irradiation. The relative positions of these levels in the gap are shown in the inset on the right-hand side of the figure. The concentration of level B in this sample is 8×10^{14} cm^{-3}, other concentrations scale with DLTS peak heights. Note the compressed scale ($\times0.25$) for $E1$ and $E2$, and the expanded scale ($\times2.5$) for $E4$ and $E5$. The DLTS rate window is 50 sec^{-1}.

region, it is the minority carrier lifetime that is the most sensitive to radiation. The lifetime is inversely proportional to the recombination rate of damage from each radiation species.

$$1/t = 1/t_o + 1/t_e + 1/t_p + \ldots \quad (15)$$

where t = minority carrier lifetime

t_o = minority carrier lifetime before irradiation

t_e = minority carrier lifetime due to electron irradiation

t_p = minority carrier lifetime due to proton irradiation

It is common to rewrite the above equation in the following form;

$$1/t = 1/t_o + K_t * \text{theta} \quad (16)$$

where theta = irradiation fluence

K_t = lifetime damage coefficient

Measuring the lifetime or diffusion length is difficult when dealing with large numbers of irradiated samples. In addition, low energy protons damage the junction space charge region that is not reflected in the minority carrier lifetime measurements. As a result, the normal method is to characterize the solar cell in terms of its output parameters; V_{oc}, I_{sc} and P_{max}. These quantities are described later in this thesis.

F. RADIATION IN THE SPACE ENVIRONMENT

The electron and the proton are the two primary radiation species of concern to the solar cell array designer. These radiations arrive at the earth after having been ejected from the Sun and carried via the solar wind. Both are trapped in the Earths magnetic field, the result being a dramatic increase in high energy charged particle density in the near Earth environment. The Earth´s magnetic field traps and accumulates electrons and protons out to approximately 10 Earth radii (64,000km). This certainly encompasses most Earth satellites.

The electron density reaches a peak at approximately 5 Earth radii(Alt 25,600km) while the proton density is at 2 Earth radii(Alt 4,750km). This is the Van Allan radiation belt [Ref. 8] and the particle density may be more than 10,000 times greater than the expected average values of charged particle density of the solar wind at 1 Au.* But this is a general description at best. The charged particle density is a function of altitude, latitude, longitude (because magnetic and polar norths differ), season, and solar activity (including solar flares). These particles are also omnidirectional and cover a broad energy range.

---

*One Astronomical unit, Au, is equal to the mean Sun-Earth distance, about 1.5E08km.

Nevertheless, mapping the radiation in "space" is an ongoing evolution.

In the laboratory it is impossible to imitate the radiation spectrum within the Earths magnetic field of influence with any accuracy. Instead, a 1-Mev electron equivalence concept has been adopted. Under this concept it is assumed that the damage caused by any radiation species of a particular energy can be added to the damage caused by another radiation species of another energy. Summing up all of these individual effects gives the total radiation damage. This accumulated damage reduces the overall performance of a solar cell. In the laboratory, a unidirectional 1-Mev electron beam that produces a similar solar cell degradation is assumed to be equivalent to the true space radiation spectrum. The validity of this concept, particularly the use of unidirectional beams verses omnidirectional beams, is currently under test by Dr Bruce Anspaugh, et al, of the Jet Propulsion Laboratory, Pasadena, California. His initial findings indicate the concept to be valid [Ref. 9].

1. Physical Features to Harden a Solar Cell

In order to slow the radiation damage in solar cells, methods to "harden" the cells have been and are being developed. To stop heavy particles and reduce the number of electrons and protons reaching the underlying solar cell, a coverglass typically made of ´fused quartz´ is affixed to

the cell's front surface. As seen in Figure 5, solar cell degradation is a strong function of coverglass thickness in proton environments. The coverglass absorbs light below 0.15um which protects the adhesive from this degrading radiation. Its overall transmittance decreases over time as the surface is literally frosted by impacting particles. In addition, impurities in the coverglass react with oxygen following excitation by radiation to form complexes that darken the coverglass.

Cell thickness is also used to harden solar cells. When radiation enters the cell material, an interaction between the radiation and the atoms may or may not occur. If the interaction is an atom displacement, then interstitial and clustering of atoms will result. These locations form electron-hole recombination centers and reduce the minority carrier's mean free path. The bottom line is a reduction in the minority carrier diffusion length. As the diffusion length decreases, so must the cell thickness to insure that current will reach the external contacts of the cell. Reducing cell thickness also reduces the probability of interaction with the incoming particle radiation, which is desirable, but it also reduces the absorption of the incoming light radiation, an undesirable effect. Because GaAs is a fragile material, reducing cell thickness and maintaining handling ease is a conflict currently under study by cell manufacturers.

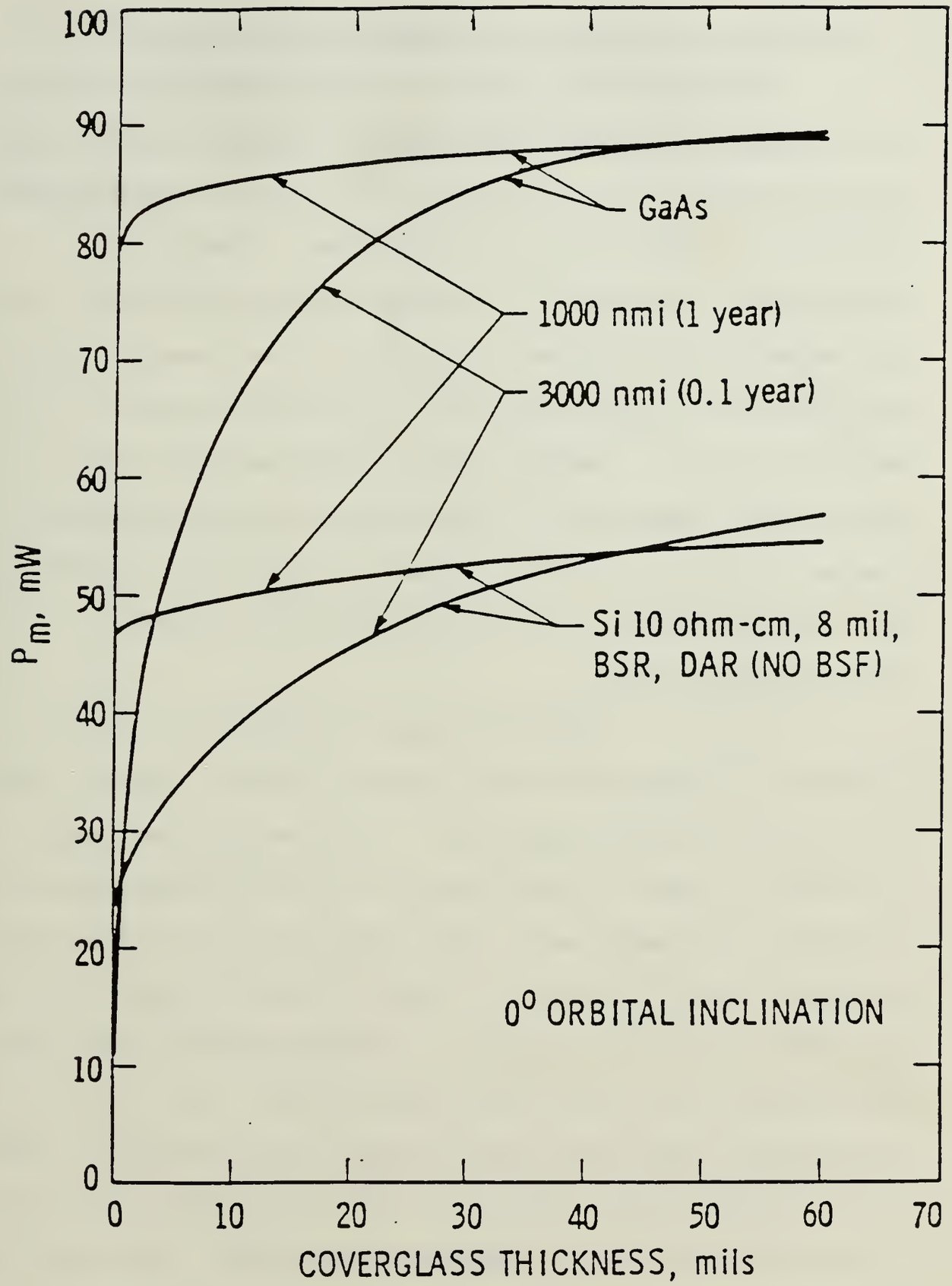

Figure 5 Computed Si and GaAs Solar Cell Power Degradation in Proton Environments [Ref. 9]

2. Chemical Features to Harden a Solar Cell

Different materials are affected differently for a given amount of particle radiation. Figures 6 and 7 gives normalized P_{max} as a function of the fluence and discrete particle energies for Silicon and GaAs. There is a significant difference in the relative damage between the two materials for proton irradiation. Low energy protons are absorbed in the coverglass of the space solar cell as seen in Figure 8. As the proton energy exceeds 1 Mev, a significant number pass through the coverglass and cause damage in the cell itself. Figure 9 shows the importance of coverglass thickness in reducing the proton damage coefficient in GaAs.

As seen in Figure 10 gallium arsenide is more radiation tolerant than the currently popular silicon as a solar cell substrate material. This one fact has been sufficient reason to cause solar cell array designers to consider using GaAs cells, even given their very high cost and handling difficulties. Tables IV and V compare Si, GaAs and other solar cell designs. Although heavier, GaAs has a much higher End Of Life (EOL) power [Ref. 10]. Table VI relates EOL power on a generic satellite with launch vehicle weight limitations. GaAs has a 60% higher EOL over Si and is slightly better than advanced Si designs. The other two designs are in the developemental stage and full scale production is some years away. Matsuda, et al [Ref. 11] has

shown that GaAs is satisfactory for space use. Zemmrich, et al [Ref. 12] report that solar cell panel assembly technology is now mature and ready for large panel construction.

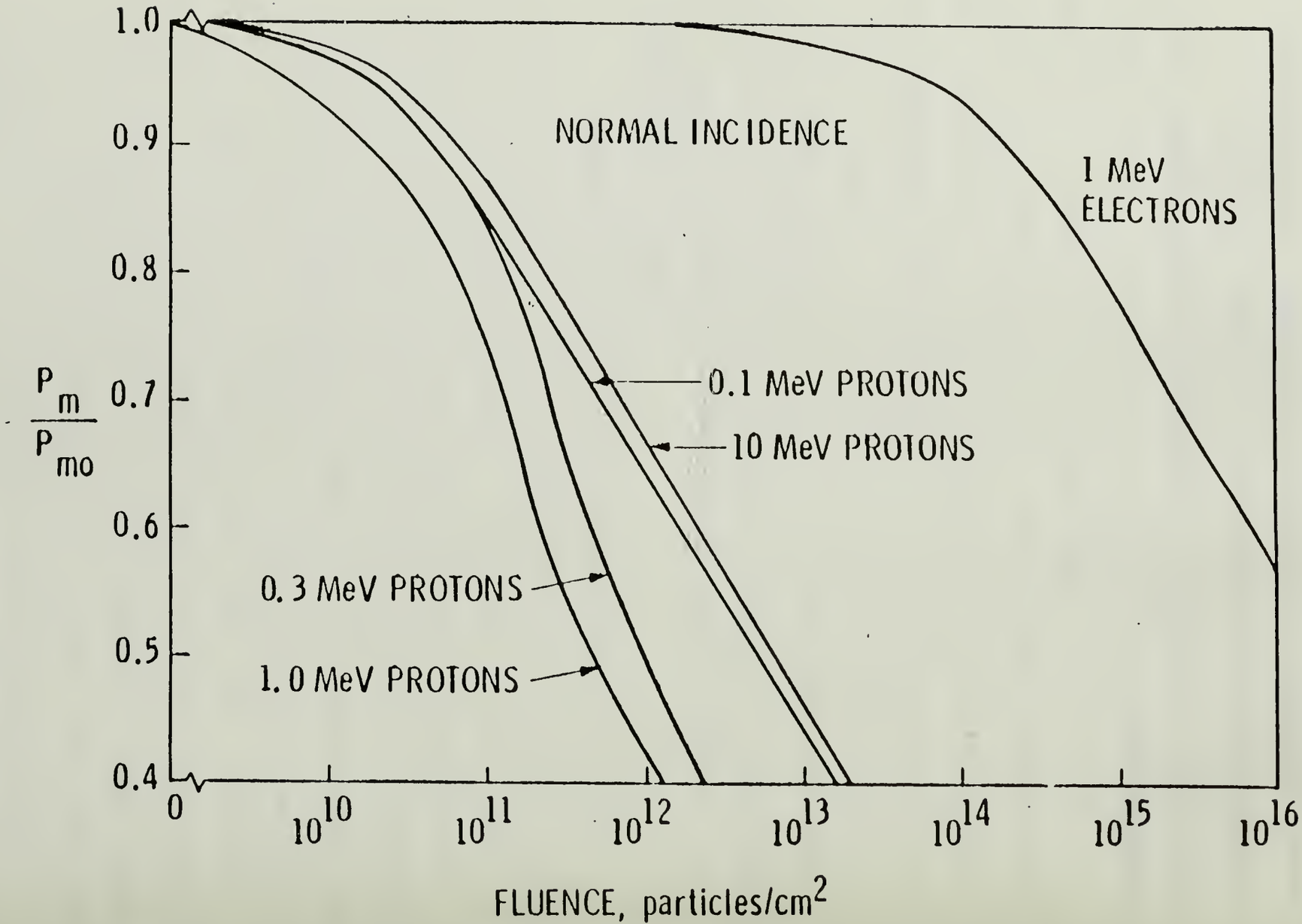

Figure 6 Particle and Energy Dependence of Silicon Pmax Degradation [Ref. 9]

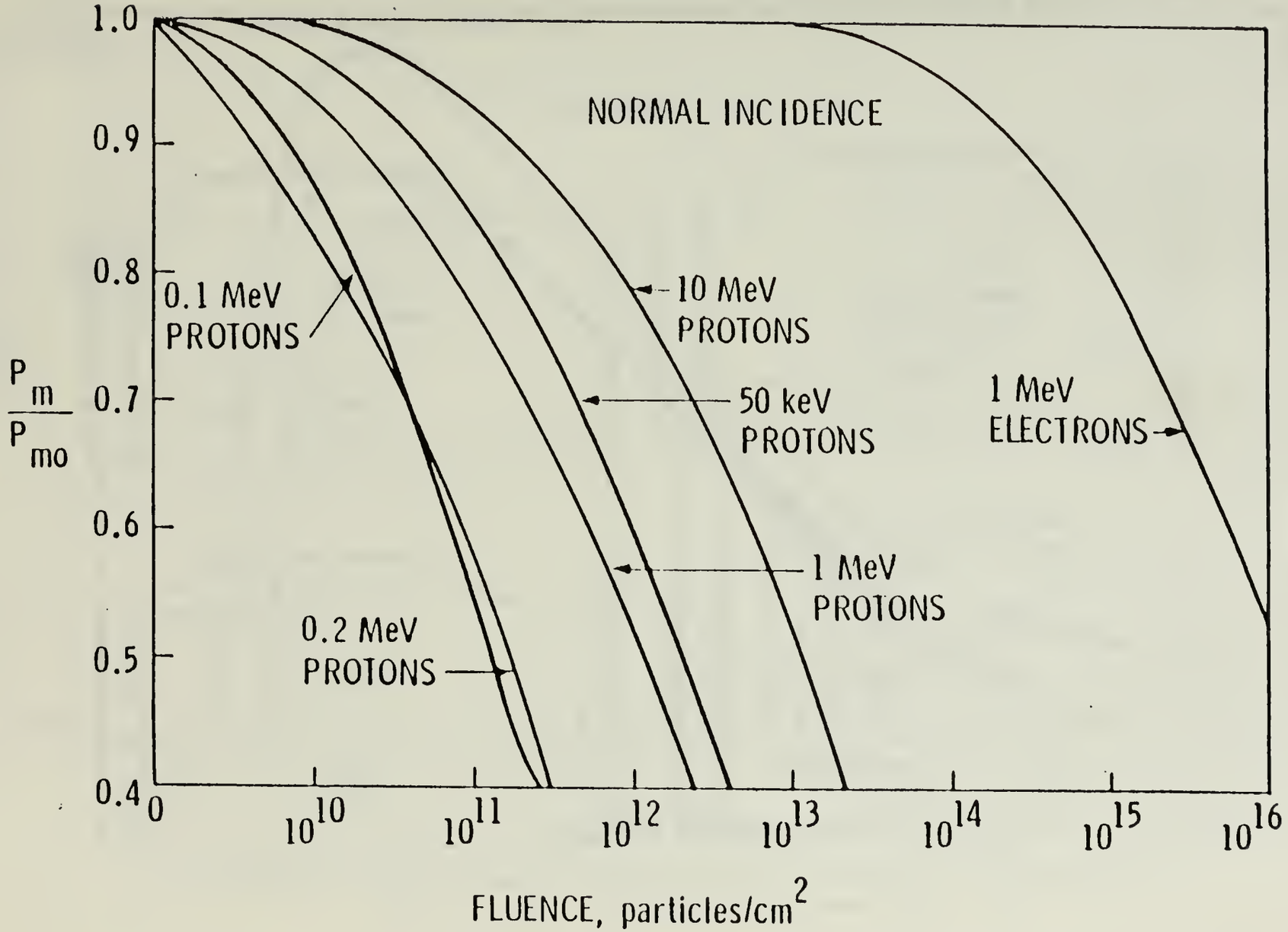

Figure 7 Particle and Energy Dependence of GaAs Pmax Degradation [Ref. 9]

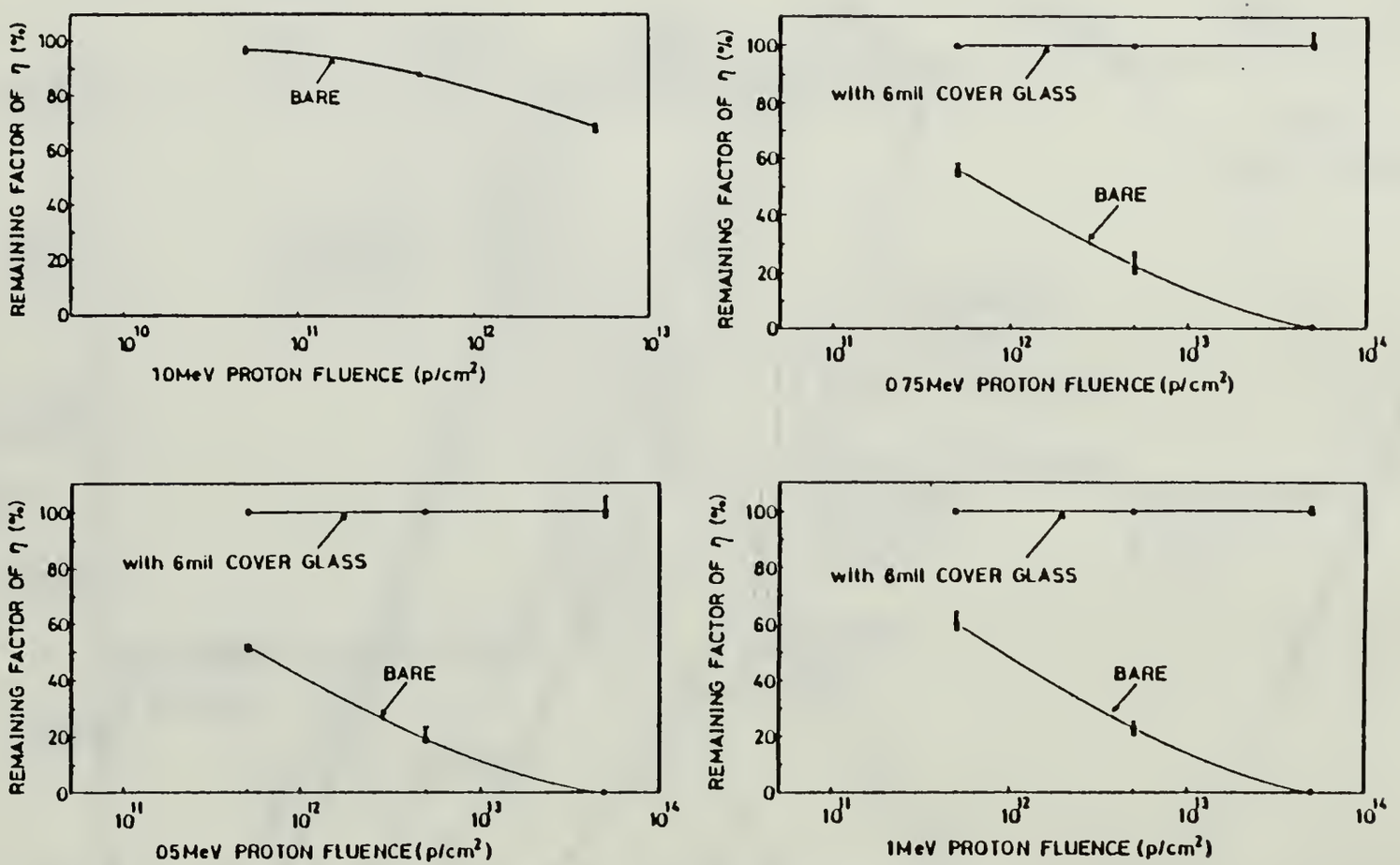

Figure 8 Efficiency Normalized to the Initial Values vs Proton Fluence [Ref. 11]

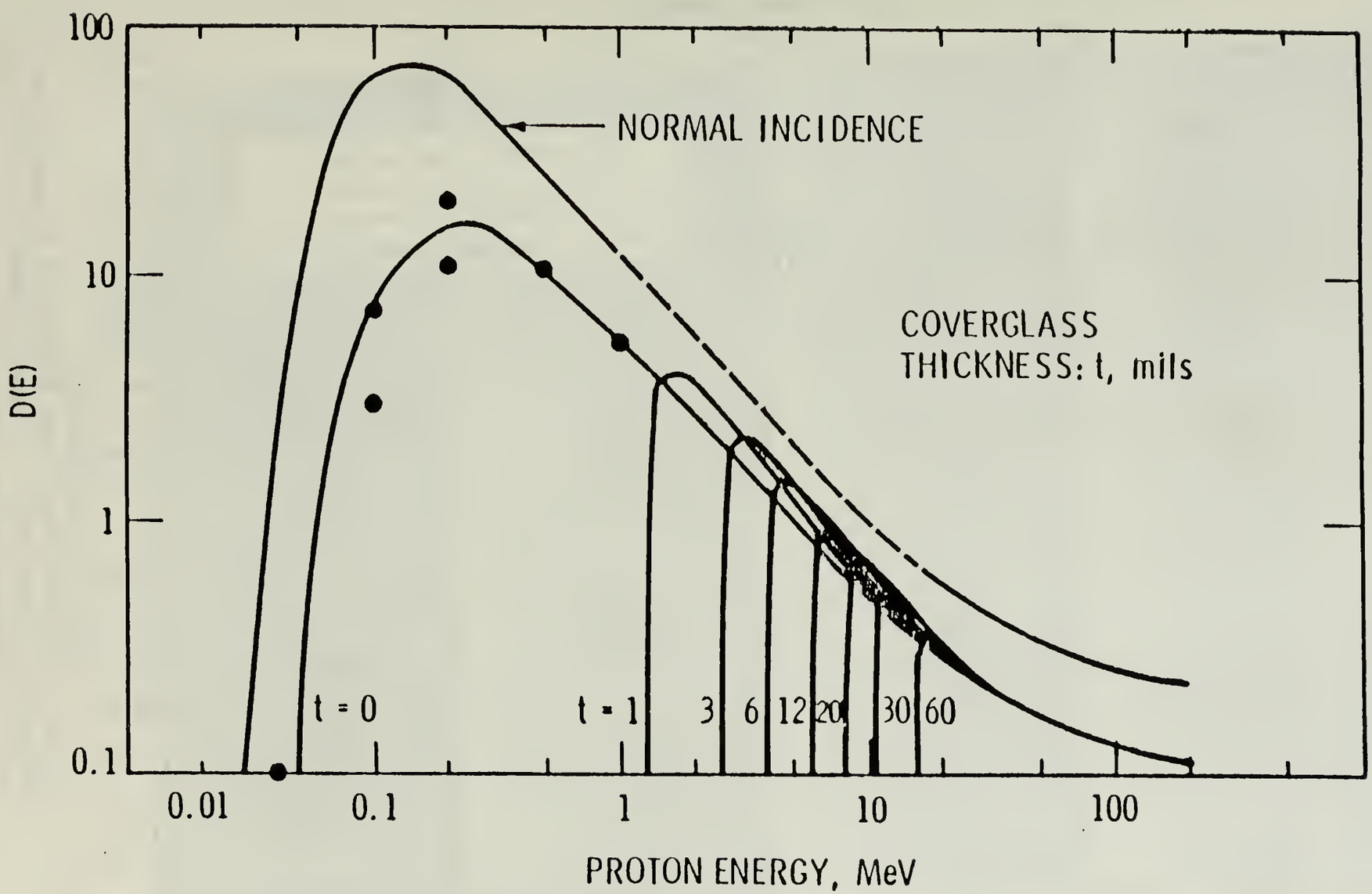

Figure 9 Pmax Damage Coefficients of GaAs as a Function of Energy and Coverglass Thickness [Ref. 9]

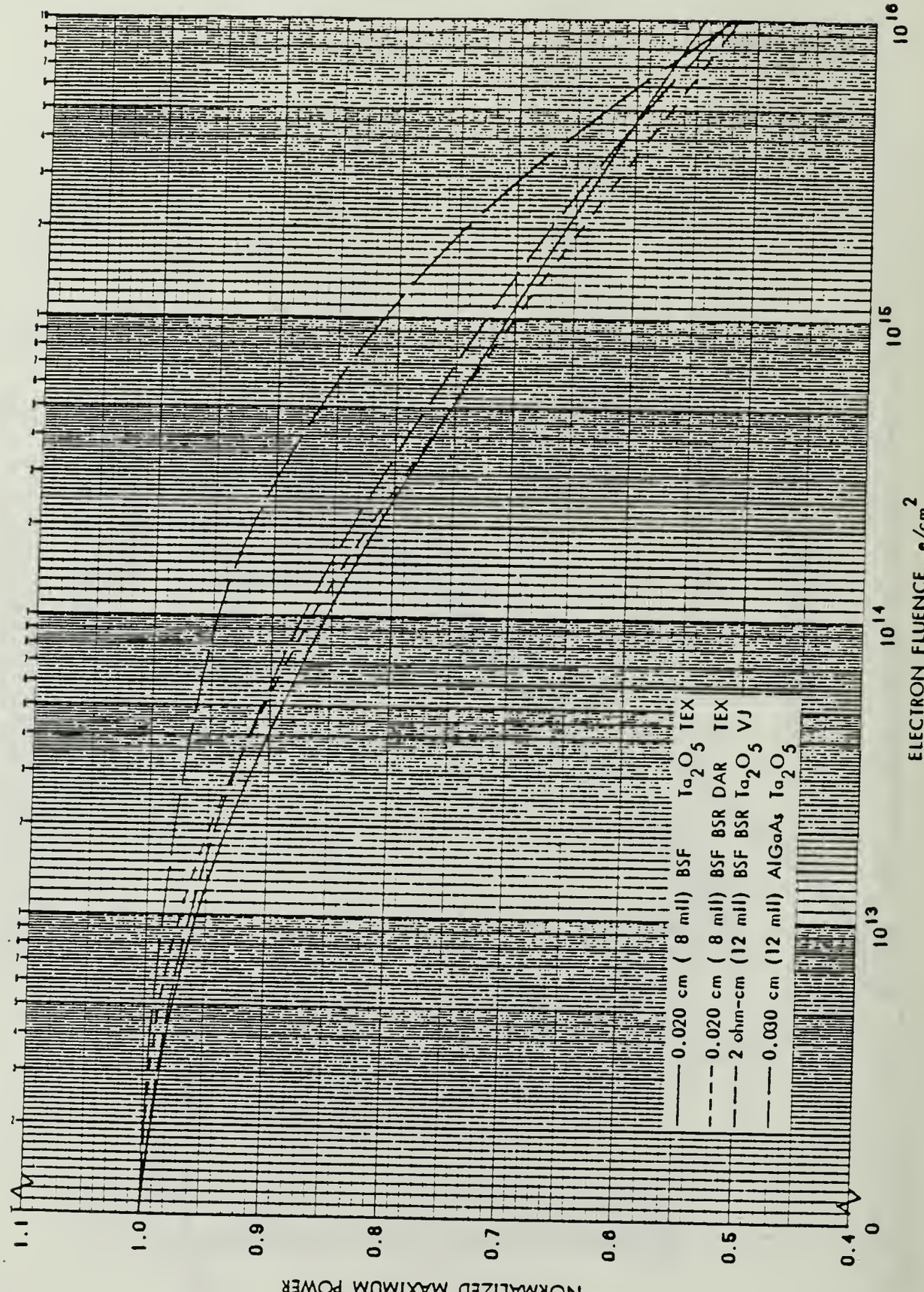

Figure 10 Normalized Pmax vs 1 Mev Electron Fluence for 10 Ohm-cm n/p Textured, 2 Ohm-cm Vertical Junction, and p/n AlGaAs Cells [Ref. 1]

TABLE IV

SOLAR PANEL TECHNOLOGY - 19,232 NM EQUATORIAL [Ref. 10]

$P_{out/unit\ area} = H_o\ N_{c25\ oC}\ K_p\ K_w\ K_r\ K_t\ K_{uv}\ K_{dm}$

SOLAR PANEL PARAMETER	SOTA Si (8 MIL)	ADV Si (2 MIL)	GaAs (8 MIL)	GALICON (2 MIL)	MULTIBANDGAP (2 MIL)
Mission Lifetime (Yrs)	5/7/10	5/7/10	5/7/10	5/7/10	5/7/10
Shield Thickness (Mils)	6	3	6	6	6
H_o = 125.7 Watts/Ft^2	-	-	-	-	-
$N_{c,\ 25^oC,\ BOL}$ (%/100)	.123	.136	.17	.17	.25
K_p (Packing Factor)	.88	.88	.88	.88	.88
K_w (Wiring Loss Factor)	.95	.95	.95	.95	.95
K_r (Rad Damage Factor)	.74/.71/.67	.67/.63/.60	.77/.73/.68	.79/.75/.70	.79/.75/.70
K_t (Temp Loss Factor)	.86	.86	.93	.93	.93
K_{uv} (UV Darkening Factor)	.97	.97	.97	.97	.97
K_{dm} (Design Margin Factor)	.98	.98	.98	.98	.98
EOL Watts/Ft^2	8/7.5/7.0	8/7.4/7.1	12/11.5/11	12.5/12/11	18.5/17.5/16.3
Solar Panel Lbs/Ft^2	.15	.07	.27	.09	.09

TABLE V

SOLAR PANEL TECHNOLOGY - 5,600 NM POLAR [Ref. 10]

$P_{out/unit\ area} = H_o\ N_{c25\ oC}\ K_p\ K_w\ K_r\ K_t\ K_{uv}\ K_{dm}$

SOLAR PANEL PARAMETER	SOTA Si (8 MIL)	ADV Si (2 MIL)	GaAs (8 MIL)	GALICON (2 MIL)	MULTIBANDGAP (2 MIL)
Mission Lifetime (Yrs)	3/5/7	3/5/7	3/5/7	3/5/7	3/5/7
Shield Thickness (Mils)	12	12	12	12	12
H_o = 125.7 Watts/Ft^2	-	-	-	-	-
N_c, 25°C, BOL (%/100)	.123	.136	.17	.17	.25
K_p (Packing Factor)	.88	.88	.88	.88	.88
K_w (Wiring Loss Factor)	.95	.95	.95	.95	.95
K_r (Rad Damage Factor)	.65/.60/.57	.62/.56/.53	.64/.56/.53	.66/.58/.55	.66/.58/.55
K_t (Temp Loss Factor)	.84	.84	.92	.92	.92
K_{uv} (UV Darkening Factor)	.99/.98/.97	.99/.98/.97	.99/.98/.97	.99/.98/.97	.99/.98/.97
K_{dm} (Design Margin Factor)	.98	.98	.98	.98	.98
EOL Watts/Ft^2	7/6.3/6.0	7.2/6.5/6.0	10.2/8.8/8.3	10.5/9.2/8.6	15.5/13.5/12.6
Solar Panel Lbs/Ft^2	.22	.15	.33	.15	.15

TABLE VI

POWER CAPABILITY VS PAYLOAD CAPABILITY [Ref. 10]
- 19,323 NM EQUATORIAL ORBIT -
(BASED ON 30% EPS WEIGHT FRACTION)

PROPULSION SYSTEM	POWER CAPABILITY (KW_e, 10 YRS EOL)				
	SOTA Si + Ni/Cd	ADV Si + IPV Ni/H_2	GaAs + CPV Ni/H_2	GALICON + HEDRB	MULTIBANDGAP + HEDRB
IUS (5000 LBS TO GEO) 1500 LBS ALLOCATED TO EPS	5	8	8	18	21
WIDE BODY CENTAUR (12,200 LBS TO GEO) 3660 LBS ALLOCATED TO EPS	12	19	19	44	50

- 5,600 NM POLAR ORBIT -
(BASED ON 30% EPS WEIGHT FRACTION)

	POWER CAPABILITY (KW_e, 5 YRS EOL)				
	SOTA Si + Ni/Cd	ADV Si + IPV Ni/H_2	GaAs + CPV Ni/H_2	GALICON + HEDRB	MULTIBANDGAP + HEDRB
IUS (8000 LBS TO MAO) 2400 LBS ALLOCATED TO EPS	8	12	13	26	33
WIDE BODY CENTAUR (13,800 LBS TO MAO) 4140 LBS ALLOCATED TO EPS	13	21	23	46	56

III. SOLAR CELL MEASUREMENT AND EVALUATION

A. COMMONLY EVALUATED SOLAR CELL PARAMETERS

Because a solar cell is simply a specially designed diode, its I-V curve looks very much like that of a diode. The curve is actually shifted negatively along current axis by an amount equal to the short circuit current, I_{SC}, as shown in Figure 11. By convention, the curve is folded

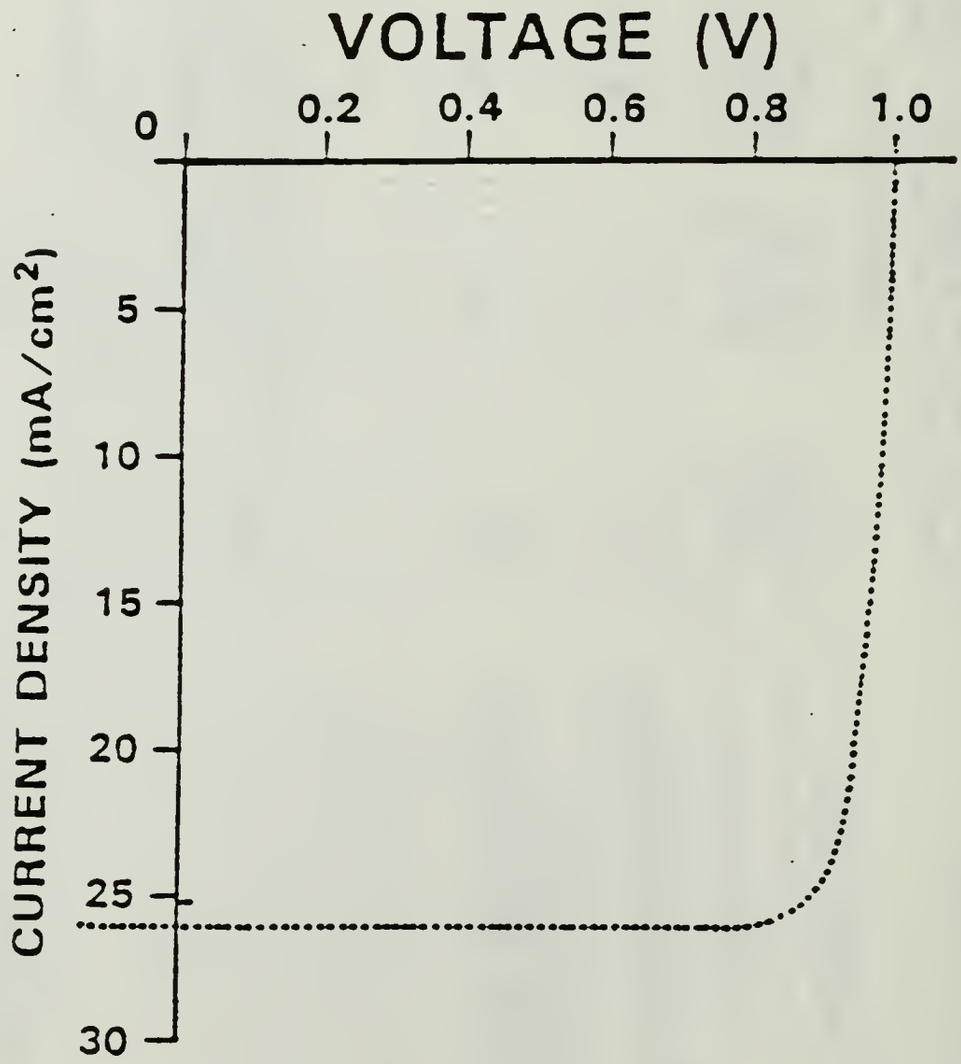

Figure 11 Photocurrent as a Function of Voltage for a GaAs Cell [Ref. 13]

about the horizontal axis so that all values are positive. Extracted or calculated from this curve are;

SHORT CIRCUIT CURRENT, I_{sc}: This is the current generated by the cell in a short circuit condition.

OPEN CIRCUIT VOLTAGE, V_{oc}: This is the voltage produced across the cell while in an open circuit condition.

MAXIMUM POWER POINT, P_{max}: The point on the curve where voltage, V_{pmax}, times current, I_{pmax}, is maximum.

$$P_{max} = V_{pmax} * I_{pmax} \qquad (17)$$

This occurs in the knee of an I-V curve.

FILL FACTOR, C_{ff}: The fill factor, given in per cent, is a measure of the squareness of the knee.

$$C_{ff} = P_{max} / (V_{oc} * I_{sc}) * 100 \qquad (18)$$

A high value for the fill factor indicates an efficient cell design, a low value, a poor design. Because the fill factor is the direct result of the cell's internal resistance, it generally changes very little with low to moderate radiation levels.

EFFICIENCY, Eff: This calculates the efficiency, in per cent, of the cell in converting photon energy into electrical energy at the maximum power point. The Air Mass zero, AM0, solar constant is 135.3mW/sq cm and the cell area must be known in square centimeters.

$$Eff = P_{max} / (135.3 * Area) \qquad (19)$$

B. SOLAR CELL PARAMETER MEASUREMENT EQUIPMENT

The AM0 light source is a Kratos SS 2500 Solar Simulator system. It produces a 10 cm diameter constant intensity beam from its Xenon arc lamp. The lens system includes a temperature controlled water filter that reduces infared (IR) wavelengths to the same levels as found in the solar spectrum.

The AM0 light is projected onto the brass solar cell test block. The test block is maintained at a constant 28 degree centigrade by circulating temperature controlled water through it. A vacuum pump is used to hold the solar cell flat on the test bed, ensuring both electrical and thermal contact to the brass fixture. Finally, two electrical leads, one from the brass test block which contacts the solar cell back surface and one from metal probes which contact the front surface of the solar cell, are available for electrical tests.

To speed up the measurement process, the I-V curves are measured using a computer controlled current sinking power supply. The computer determines the voltage range of the solar cell then steps the power supply through this range, measuring the corresponding current. The computer stores this information along with the calculated electrical power for this point.

All data can now be transferred to floppy disk. Once on floppy disk, the data can be retrieved and plotted on an X-Y

plotter. Additional information on the hardware configuration, driving software and light parameters can be found in reference 14.

C. SOLAR CELL RADIATION EQUIPMENT

The solar cell radiation damage for laboratory work is caused by an electron linear accelerator (LINAC). This equipment consists of four main sections. They are 1) the electron gun which produces multi-energetic electrons and focuses them at the output stage; 2) the accelerator section which uses an alternating potential to speed up the electron beam. Those electrons which do not have the proper energy to 'sync' with this alternating potential will be lost; 3) a deflection section which turns the electron beam through a particular radius of curvature using a magnetic field. Only those electrons having a narrow energy range emerge from this section. And 4) the final section is the target chamber. The Naval Postgraduate School, NPS, uses a fixed target with a beam that measures up to 3cm by 3cm. JPL in Pasadena, CA uses a fixed or oscillating target with beams up to 14cm in radius. In wider beams. The electron intensity falls off toward the beam edges by a much as 12% of the beam center value.

The interior of the target chamber is under very low pressure, and in general, the radiation of solar cells occurs under dark conditions.

The NPS LINAC produces 20 Mev to 100 Mev electrons while the JPL system, known as a Dynamitron accelerator, produces 1 Mev electrons. As stated earlier, 1 Mev electrons are the accepted standard for equivalent radiation for space applications.

IV. SOLAR CELL ANNEALING

A. ANNEALING TYPES

The strict definition of annealing is: "the heating and slow cooling of a metal (or glass) to reduce its brittleness". This reduction in brittleness is not the desired result of solar cell annealing. Perhaps the term annealing is inappropriate here, but it now has common usage. A much better definition would be:

Solar Cell Annealing - The temporary introduction of energy into a solar cell that causes recovery of desirable electrical properties lost due to radiation damage.

An earlier section described how radiation, either man-made or space borne, causes lattice damage to the solar cell and thereby reducing its electrical power production capability. Although reduced, this capability is not lost.

An analogy can be drawn with the rechargeable battery. The battery starts its life with an inherent amount of usable power available. The battery's very use causes chemical changes within itself that reduce the available power. Once the battery has discharged to a point that it is no longer useful it must be recharged, perhaps with an electrical current. Although recharging does not return the

battery to 100% of its initial (new) state, recovery is significant (and inexpensive) enough to warrant the effort.

In the solar cell, radiation damage reduces the power production capability. The cell can reach a point where it is no longer useful in providing power to the spacecraft. If the spacecrafts' primary power source is the solar cell array, then the spacecraft is useless. Introduction of energy from one of several outside sources can rejuvenate the solar cell to within a large fraction of its original capability. These rejuvenation methods are thermal annealing (heating the cell) and minority carrier injection annealing (by forward bias current or intense light).

1. Thermal Annealing

Thermal annealing is by far the most familiar method for affecting solar cell recovery. The thermal energy allows radiation damaged lattice structures to redistribute interstitials and clusterings to form a more regular lattice and thereby reduce the recombination centers. In general the speed of the recovery is proportional to the temperature of the cell but so is dopant diffusion. The trick is to cause cell recovery to occur as rapidly as possible and at the same time not allow a significant degradation of the P-N junction due to diffusion of the dopants away from the junction. GaAs solar cells anneal satisfactory in the 200-300 degree centigrade range while Si solar cells require 300-400 degrees centigrade. All components of the solar

array panel must be capable of withstanding the annealing temperature. Adhesives used to attach cover glasses to cells and cells to substrate structures begin to fail around 450 degree centigrade. This fact plus the additional energy required for Silicon´s higher temperature make GaAs the first choice for on-orbit thermal annealing. Another consideration is the electrical contact material. Soldered contacts currently in use will melt causing loss of contacts around 190 degrees centigrade, certainly unacceptable for GaAs annealing.

2. Minority Carrier Injection Annealing

Minority carrier injection is the second method of annealing. A large current density, perhaps 10 to 100 times greater than the solar cells ´normal´ current density, is created in the cell. When an electron and hole are lost at a recombination center there is an initial transfer of electronic energy into short-lived violent local vibrations of the defect. It is this vibration that allows defect motion to occur. In fact, movement on the order of a lattice constant is possible. Normally this would require 1.4ev of thermal energy to cause such movement. This implies that there is very strong electron-lattice coupling at the defect site. One would suspect that increasing both the current density and the temperature would increase the annealing rate of the individual methods. This data is not published and in fact may still need to be collected

experimentally. There are two methods of minority carrier injection, Photo-injection and Forward-bias injection.

a. Photo-injection Annealing

Photo-injection requires that an extremely powerful light be directed on the solar cell's front surface. This inturn produces a very large minority carrier density, which then promotes damage recovery. The light source could be from a laser or large solar concentrators.

A great deal of work is currently being conducted in the solar cell array concentrator area. Each cell would have its own large area concentrator which would focus the solar energy onto a much smaller solar cell. The driving force behind this work is to sharply increase the power density of an array. This system could actually perform Photo-injection annealing continuously while also providing the spacecraft with power. Additionally, the concentrator acts as a radiation barrier, significantly reducing the radiation reaching and damaging the solar cell. But the concentrator system has its own problems; high pointing accuracy requirement, surface degradation due to bombardment, extra space and weight during launch, reliability of deployment once in orbit, susceptibility to direct laser kill, cell efficiency loss due to elevated temperatures, and others.

b. Forward-bias Current Annealing

The other method is Forward-bias current annealing. Here a forward-biased potential is placed across the solar cell junction to force a large current through it. Because of the diode nature of the P-N junction, once a forward current begins to flow, a small increase in the forward potential increases the forward current dramatically due to the exponential relationship. The power dissipated in a typical resistor type device is proportional to the current squared; which is not the case in semiconductor due to their non-linear characteristics.

$$I = I_o * (\exp((V - V_d)/V_T) - 1); \quad (20)$$

where $V_T = k*T/q$ and $V >= V_d$

$$V = V_T * \ln(1 + I/I_o) + V_d \quad (21)$$

$$P = I * V \quad (22)$$

$$= I * (V_T * \ln(1 + I/I_o) + V_d) \quad (23)$$

$$P/I_o = (I/I_o) * (V_T * \ln(1 + I/I_o) + V_d) \quad (24)$$

Plotting current, I/I_o, vs. voltage, V, for $V > V_d$ gives the typical I-V curve for a diode under forward bias. A plot of the current, I/I_o, vs. power, P/I_o, produces a straight line for values $I/I_o < 500$ of slope K. In fact, K is a very slow changing function of I/I_o and for large range can be considered constant.

$$P/I_o = I/I_o * K; \text{ or} \quad (25)$$

$$P = I * K \quad (26)$$

The power dissipated in the solar cell is proportional to the current flow; therefore, heating of the cell is proportional to the current. An alternate heating source may be required to combine thermal and current annealing and thereby increase the annealing rate. In Figure 12 the measured surface temperature, T, of a 2cmX2cm GaAs solar cell is compared to the forward bias current. The measurement was run over three ambient temperatures. Although this figure would not be representative of any spacecraft array, it shows that continuous forward bias current will tend to linearly raise the array temperature.

B. PREVIOUS ANNEALING WORK

Early work done by Lang, et al, [Refs. 15, 16, 17] on semiconductors made of GaAs and GaP has shown that these materials anneal readily at low temperatures using a forward bias current. Using low current densities on the order of 0.5 to 2.0el/cm^2, they realized recovery time constants in the 1Hr to 2Hr range for the two of the electron traps, E1 and E2 [see section on DLTS in this thesis]. Current data indicates that traps E1 and E2 anneal at the same rate while traps E3, E5 and H1 anneal at the same rate.

This work was extended to the solar cells by Loo, et al [Ref. 18], Stievenard, et al [Ref. 19] and a few others. The early work done by Loo involved thermally annealing the solar cell at 200 degrees centigrade for several days until

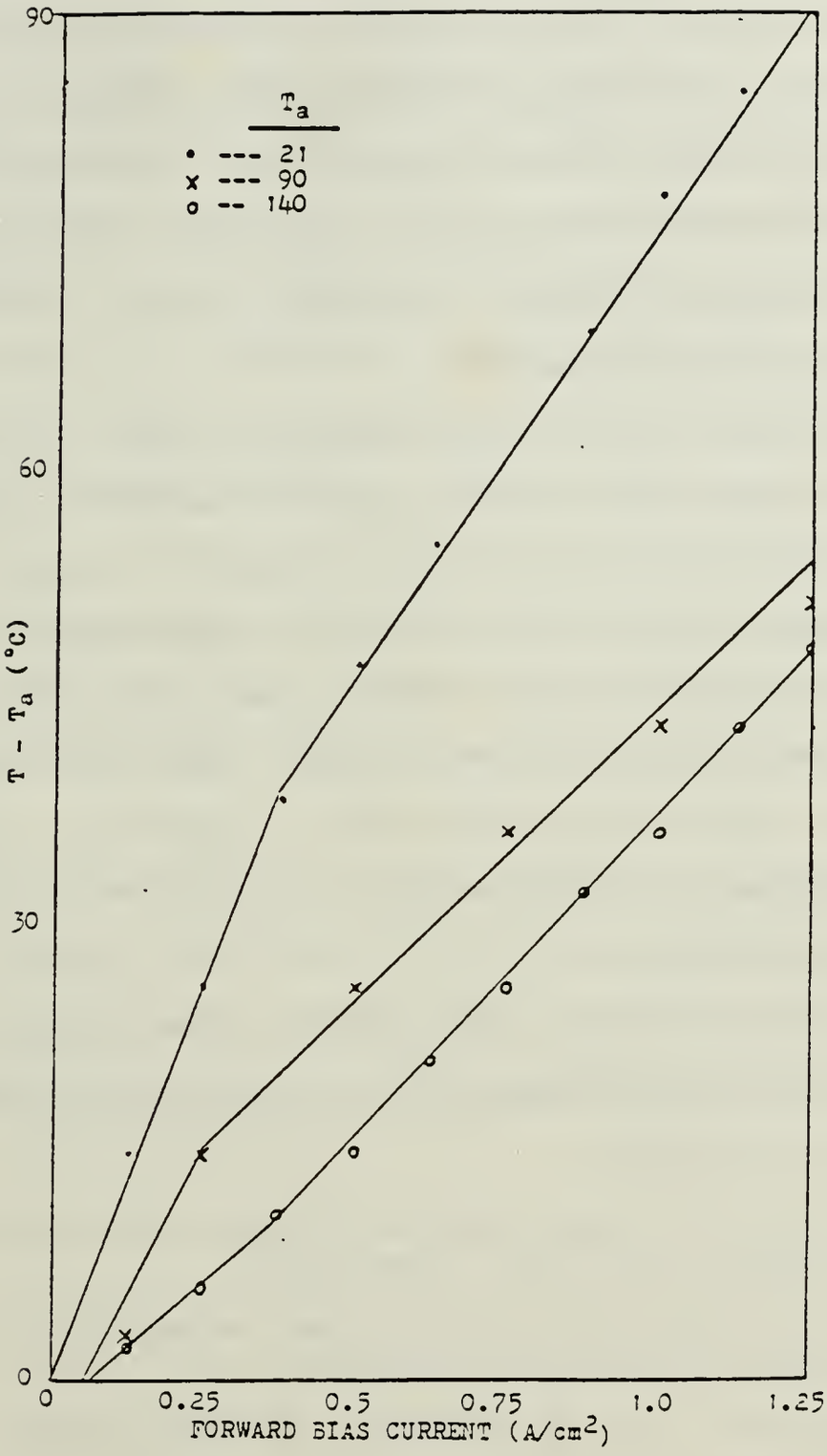

Figure 12 Cell Temperature, T, vs. Forward Bias Current as a Function of Ambient Temperature, T_a.

the anneal rate approached zero. Cells generally recovered to 80% of their pre-irradiated values using this procedure. The forward bias current was then introduced, while maintaining the elevated temperature. The solar cells were then annealed for several more days using the procedure. The combination produced a recovery to 90% of its pre-irradiation values.

Stievenard did not pre-thermally anneal the solar cells. Temperature of the cells were maintained at 60 degrees centigrade and a forward bias current of 1.3A/cm^2 was used. Stievenard reported only the time constant of the E5 trap which was about 2 hours. This current density is three times greater than that used by Loo, implying a shorter time constant than would be expected at 0.5A/cm^2. This proved that low temperature annealing was possible in the delicate GaAs solar cell.

This does indicate that current annealing has possible value for on-orbit annealing, but it does not answer two important questions;

1) Does simultaneous use of thermal and current annealing increase the anneal rate? And,

2) Can current annealing be used successfully at temperatures found on-orbit?

Question 2 will be addressed in the remainder of this thesis. There are several reasons that this annealing system is appealing. First, this system is essentially electronic and not mechanical thereby keeping weight and

complexity to a minimum. During periods of low energy requirements, the excess current generated could be directed to an array section until needed for operational reasons. Second, the temperature of the solar cell arrays while on-orbit typically reach 100 degrees centigrade. This is ´FREE´ energy. Array temperatures could also be increased by adjusting passive radiation systems during the annealing period. And third, annealing a section of an array does not effect the remainder of array. Raising the array temperature to 200 degrees centigrade or more during thermal annealing reduces the efficiency of the entire array. Not so for current annealing, although the section undergoing annealing will be lost from the power grid during the process.

Although GaAs will not anneal thermally at temperatures below 200 degrees centigrade, the kT energy available in the solar cells due to the ambient array temperature may contribute to annealing once a forward-bias current starts to pass.

V. FORWARD-BIAS CURRENT ANNEALING EXPERIMENT*

A. PRE-ANNEAL SOLAR CELLS

Five GaAs solar cells, E-6 through E-10, were obtained that had been irradiated continuously with 1-Mev electrons by JPL for a total fluence of 3E15e1/cm^2. An additional four cells, E-20, E-22, E-23 and E-24, were obtained that had been irradiated continuously with 1-Mev electrons for a total fluence of 1E15e1/cm^2.** These cells were manufactured in 1985 using OM-CVD production line techniques by Applied Solar Energy Corporation under Airforce Materials Laboratory contract F33615-81-C-5150. Cross-sectional data of a cell is shown in Table VII and Figure 13.

I-V curves for each cell were produced using the NPS Solar Simulator laboratory. The output parameters measured were compared to the post irradiation data provided with the cells so that correction factors could be calculated and used later if needed. All output parameters were within a few percent of the post irradiation values. On the other hand, the variation in cell parameters from cell to cell appears large. A comparison with Figures 14 and 15 dispute

---

*See Appendix A for pre-experimental trials.

**Appendix B describes the experiment conducted with cells E-22 and E-23.

TABLE VII

ASEC P/N 2cm X 2cm GaAs SOLAR CELLS

Substrate thickness	300 uM
N layer thickness	9 uM
P junction layer thickness-Zn doped	0.5 uM
P window - $Al_xGa_{1-x}As$ ($x \sim .86-.9$) thickness	0.1 uM
P contact material	Au - Zn - Ag
N contact material	Au - Ni - Ge - Ag
Anti-reflection coating	TiO_2, Al_2O_3

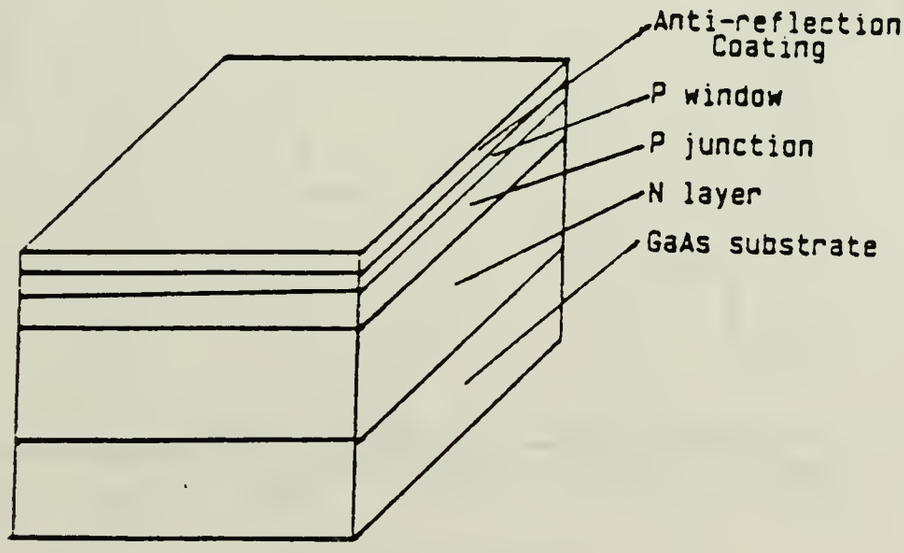

Figure 13 Cross-Sectional View for the ASEC AlGaAs-GaAs Used in this Thesis

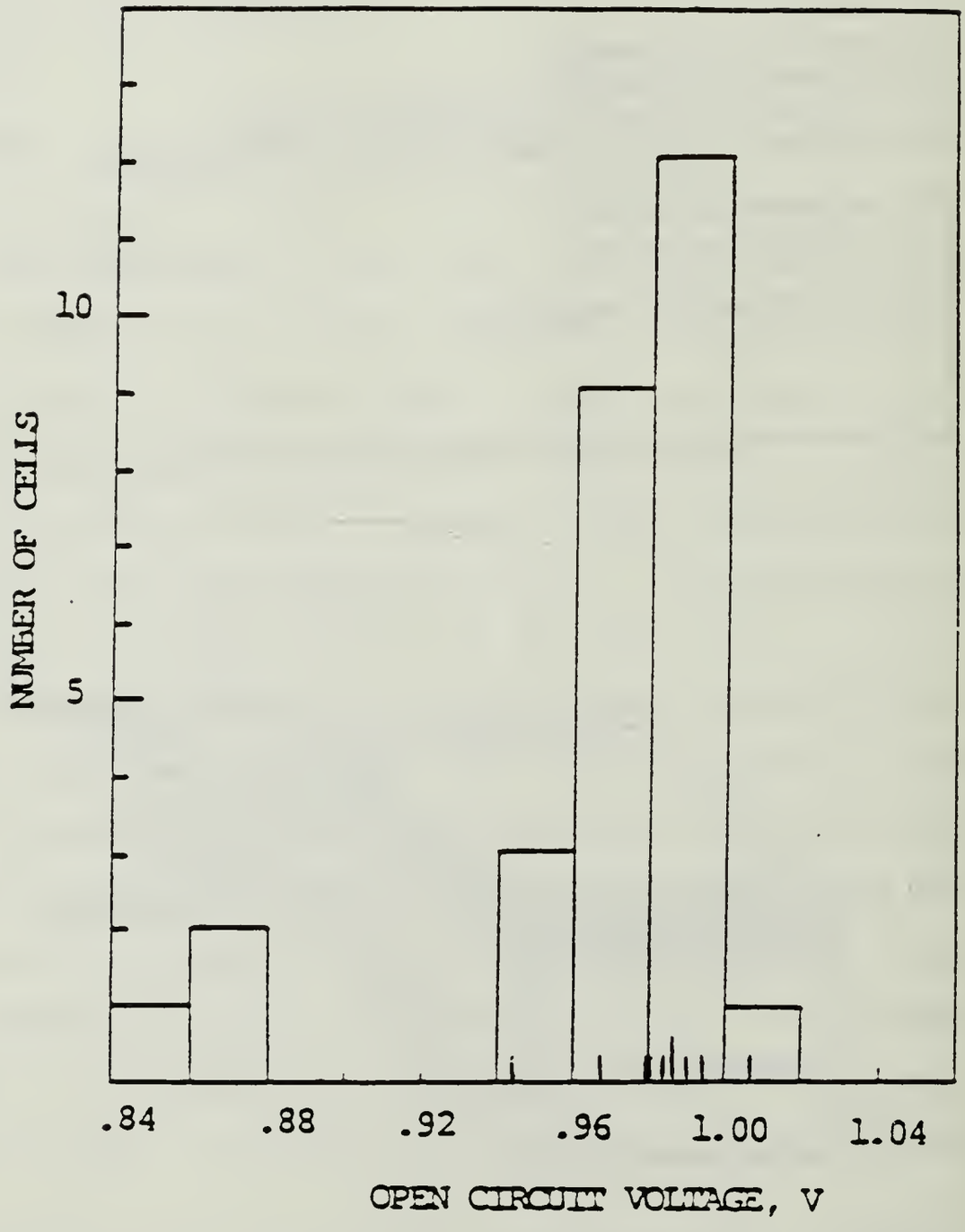

Figure 14 Histogram of Open Circuit Voltage for GaAs Production Run [Ref. 20]

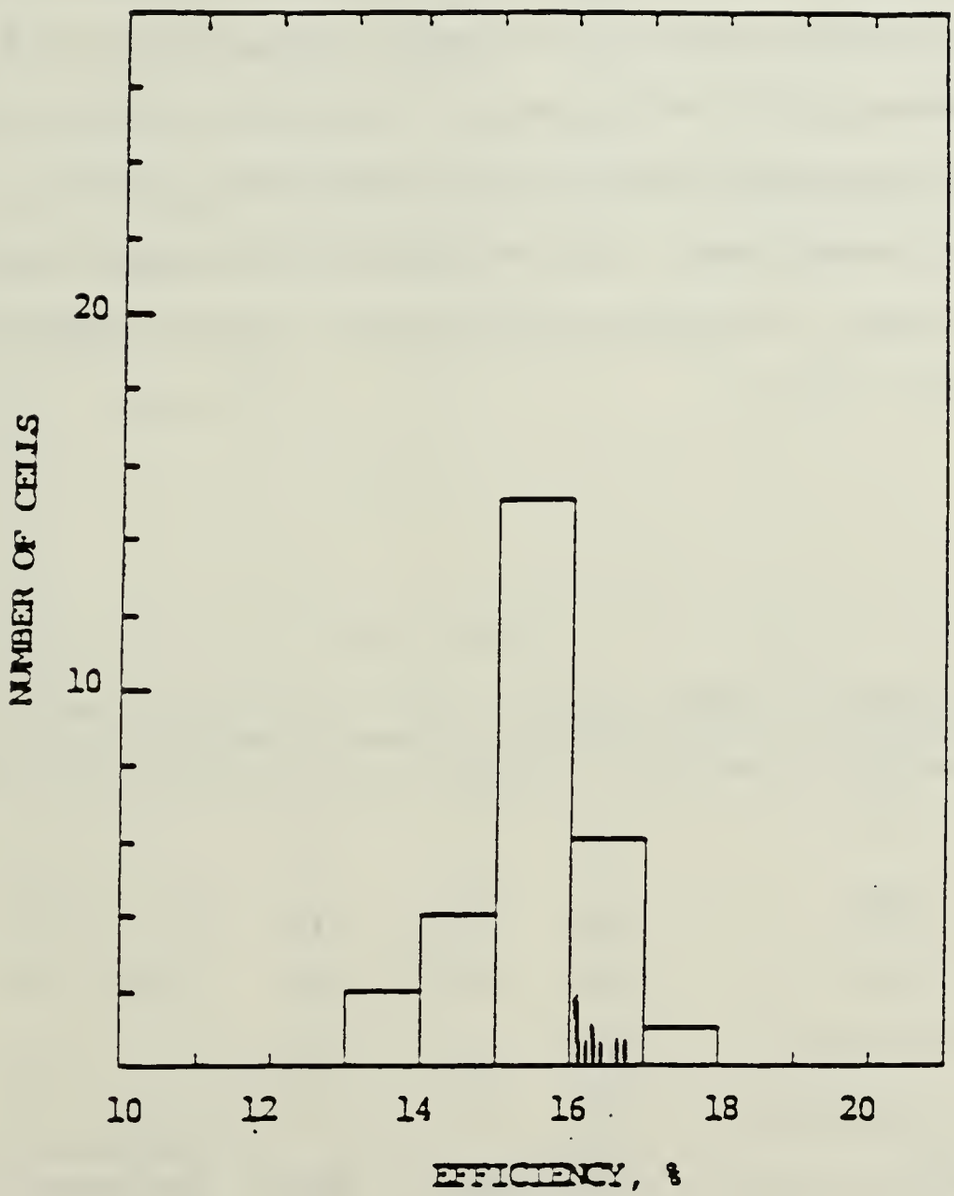

Figure 15 Histogram of AM0 Efficiency for GaAs Production Run [Ref. 20]

this. These two figures are histograms of a production run of GaAs solar cells. The cells used are all centered in the upper ranges of the histograms.

B. ANNEALING PROCEDURE

One cell, E-20, was used as a control sample. It was placed in the oven at 90 degrees centigrade for 35 hours in an open circuit configuration. As with all cells during this experiment, the cell was illuminated with an incendescent lamp of 75W that approximated AM1 solar conditions. As seen from Table VIII thermal annealing did not take place.

TABLE VIII

EXPERIMENTAL CONTROL CELL. 2cm X 2cm GaAs solar cell E-20 continuously irradiated with 1-Mev electrons for a total fluence of 1E15e1/cm^2. Temperature was held at 90 degrees centigrade.

TIME (hrs)	V_{OC} (mV)	I_{SC} (mA)	C_{ff} (%)	V_m (mV)	Eff (%)	P_{max} (mW)
Pre-irradiated	944	120	76.9		16.1	87
Post-irradiated	894	100	79.4	780	13.0	71
Check-in, (0Hrs)	889	100	80.0	765	13.2	71
35	891	102	78.9	747	13.3	72

Four cells, E-6, E-7, E-9 and E-10, were then current annealed for various lengths of time at 2 amps, or 0.5 amps per cm^2.* At regular intervals during the annealing process, the cells were removed from the oven, cooled to 28 degrees centigrade and electrical parameters measured. Tables IX through XII compile this data for the different cells. Figures 16 and 17 show the life history of cells E-9 and E-10 in terms of their I-V curves. In all parameters, except C_{ff} and $V_{m'}$ improvement falls off with time. C_{ff} should not change as explained earlier. The sudden shift of V_m to the left at the 42 and 48 hour points in cells E-9 and E-10 was not expected.

---

*The annealing was ended at various levels to allow follow on testing. When the experiment was in progress, it appeared that both a DLTS and visible spectrum analyzer would be available. Unfortunately both equipments were inoperable when the annealing experiment ended. The four solar cells have been retained for possible future testing using these systems.

TABLE IX

CURRENT ANNEALED SOLAR CELL E-6. 2cm X 2cm GaAs solar cell E-6 continuously irradiated with 1-Mev electrons for a total fluence of 3E15el/cm^2 then annealed using 0.5 Amps/cm^2. Ambient temperature during anneal was held to 90 degrees centigrade.

TIME (hrs)	V_{OC} (mV)	I_{SC} (mA)	C_{ff} (%)	V_m (mV)	Eff (%)	P_{max} (mW)
Pre-irradiated	984	119	74.8		16.2	88
Post-irradiated	873	84	78.8	748	10.7	58
Check-in, (0Hrs)	871	85	79.7	757	11.0	59
6	878	87	80.4	761	11.4	62

TABLE X

CURRENT ANNEALED SOLAR CELL E-7. 2cm X 2cm GaAs solar cell E-7 continuously irradiated with 1-Mev electrons for a total fluence of 3E15el/cm^2 then annealed using 0.5 Amps/cm^2. Ambient temperature during anneal was held to 90 degrees centigrade.

TIME (hrs)	V_{OC} (mV)	I_{SC} (mA)	C_{ff} (%)	V_m (mV)	Eff (%)	P_{max} (mW)
Pre-irradiated	1008	115	78.6		16.8	91
Post-irradiated	875	73	80.6	772	9.5	51
Check-in, (0Hrs)	873	72	81.6	762	9.5	51
6	882	76	82.2	776	10.2	55
24	890	81	82.3	779	11.0	59

TABLE XI

CURRENT ANNEALED SOLAR CELL E-9. 2cm X 2cm GaAs solar cell E-9 continuously irradiated with 1-Mev electrons for a total fluence of 3E15el/cm^2 then annealed using 0.5 Amps/cm^2. Ambient temperature during anneal was held to 90 degrees centigrade.

TIME (hrs)	V_{OC} (mV)	I_{SC} (mA)	C_{ff} (%)	V_m (mV)	Eff (%)	P_{max} (mW)
Pre-irradiated	980	119	74.9		16.1	87
Post-irradiated	865	75	79.2	752	9.5	51
Check-in, (0Hrs)	862	73	80.2	739	9.3	50
6	872	76	81.0	756	9.9	53
18	876	80	81.2	786	10.6	57
42	882	86	80.0	758	11.2	61
48	880	87	78.9	759	11.2	60

TABLE XII

CURRENT ANNEALED SOLAR CELL E-10. 2cm X 2cm GaAs solar cell E-10 continuously irradiated with 1-Mev electrons for a total fluence of 3E15e1/cm^2 then annealed using 0.5 Amps/cm^2. Ambient temperature during anneal was held to 90 degrees centigrade.

TIME (hrs)	V_{OC} (mV)	I_{SC} (mA)	C_{ff} (%)	V_m (mV)	Eff (%)	P_{max} (mW)
Pre-irradiated	996	120	74.0		16.3	88
Post-irradiated	875	84	80.1	748	10.9	59
Check-in, (0Hrs)	873	85	80.2	747	11.0	59
6	879	87	80.4	776	11.4	62
18	883	90	80.3	769	11.8	64
42	889	93	79.9	767	12.3	66
48	891	95	79.3	753	12.4	67
72	892	95	78.9	756	12.4	67
96	892	97	77.5	758	12.4	67

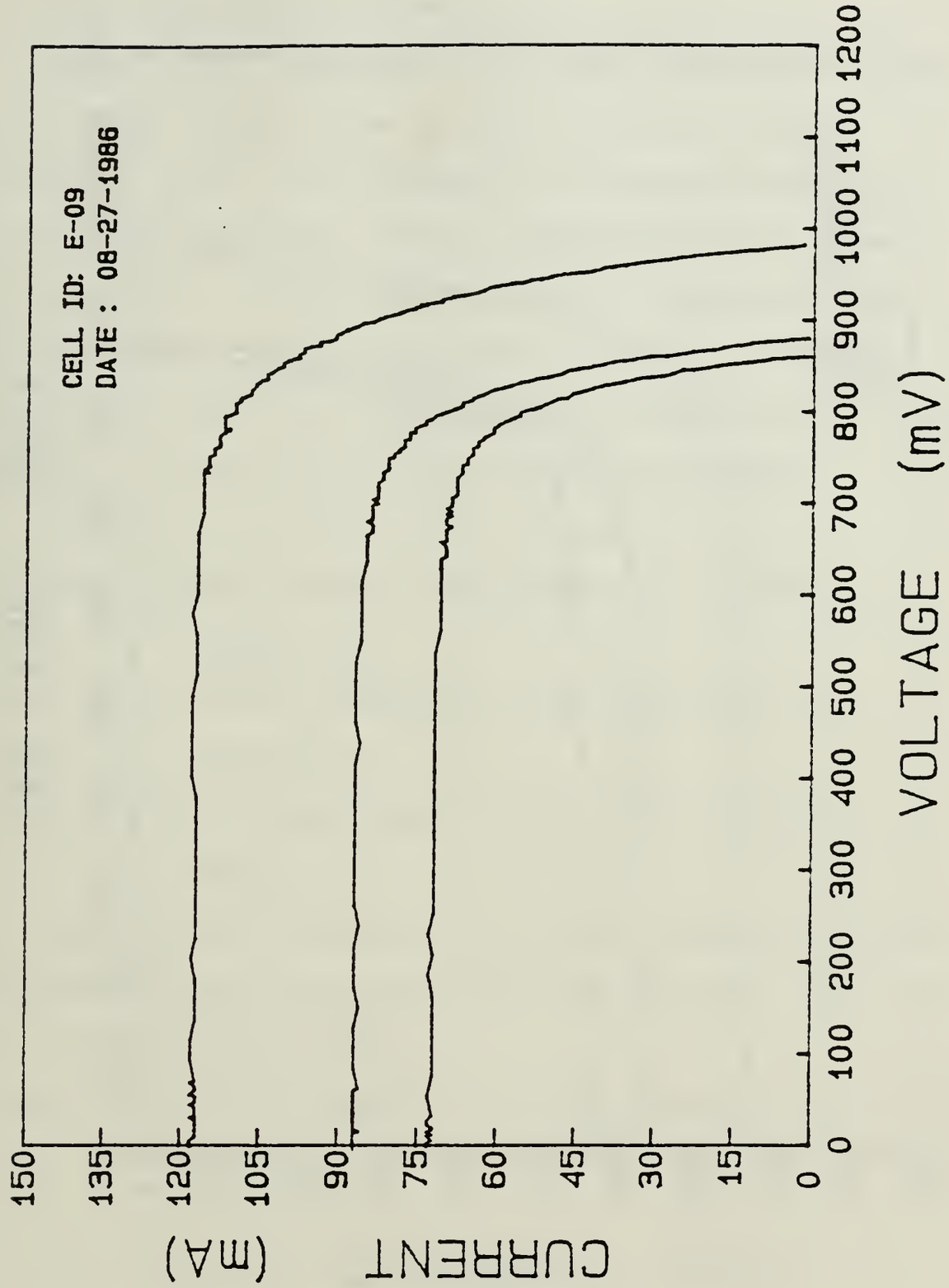

Figure 16 I-V Curves for GaAs Solar Cell E-9 Showing Pre- and Post-irradiation and Post-anneal Values

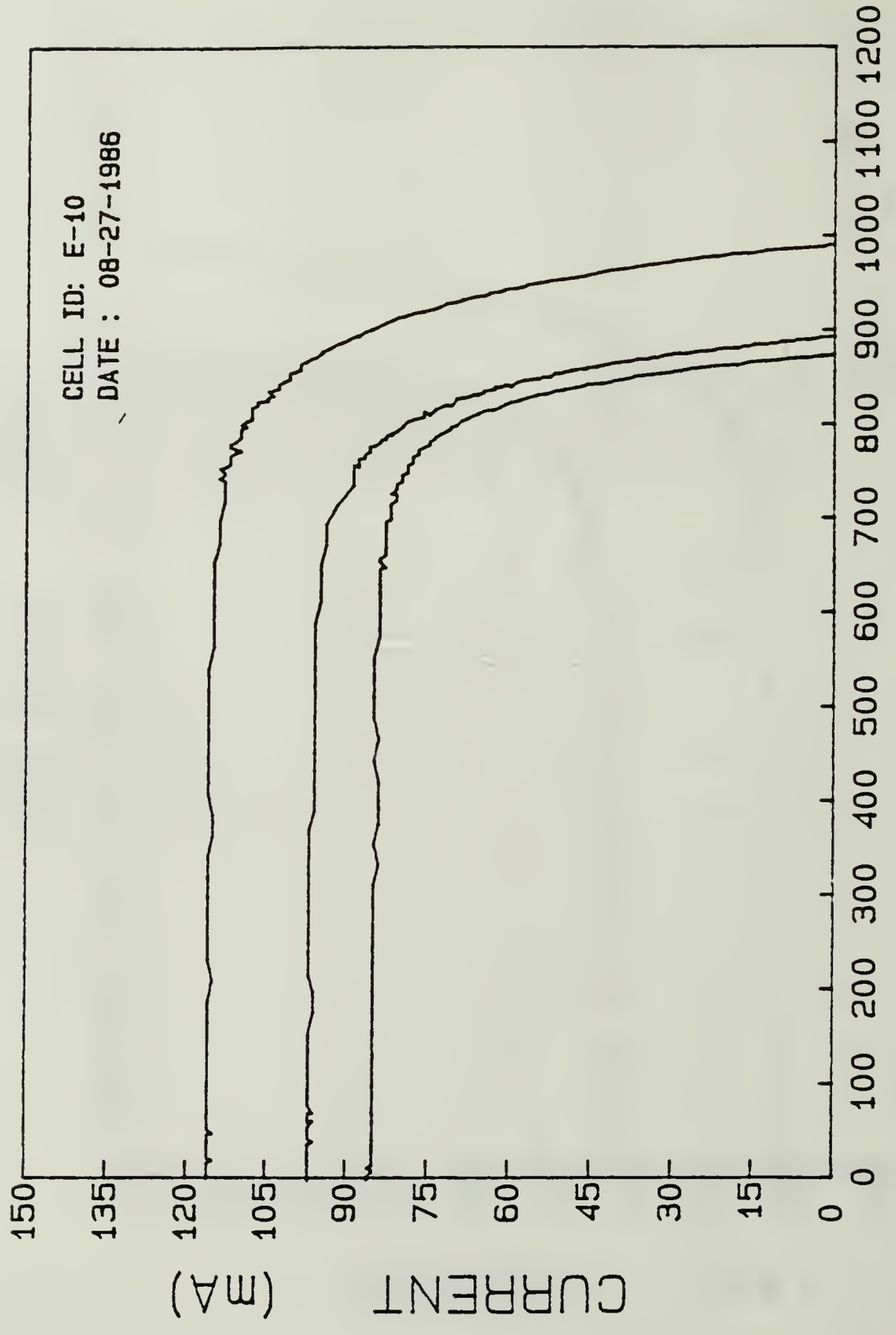

Figure 17 I-V Curves for GaAs Solar Cell E-10 Showing Pre- and Post-irradiation and Post-anneal Values

C. POST-ANNEAL CALCULATIONS

Normally, on spacecraft, the power conditioning system operates in the P_{max} area of the solar cell array. Therefore, this is the parameter of primary interest on orbit. An attempt was made to empirically fit a curve to the P_{max} data. It was assumed that any improvement in P_{max} would be proportional to the amount of damage remaining in the cell and that each damage mechanism would anneal at its own rate. This results in the following equation;

$$P(t) = P - a_1*\exp(-t/L_1) - a_2*\exp(-t/L_2) - \ldots \quad (27)$$

where a_1, a_2 are related to the amount of a particular damage, and

L_1, L_2 are the respective time constants for annealing.

P is the maximum power obtained when annealing stopped.

There are five unknowns in the above equation and each additional exponential term would add two more. The anneal rate is calculated using;

$$dP(t)/dt = (a_1/L_1)*\exp(-t/L_1)+(a_2/L_2)*\exp(-t/L_2)+\ldots \quad (28)$$

Using the data from Table XII in Equation 27 leads to the following;

$$59 = P - a_1 - a_2$$

$$62 = P - a_1 * X - a_2 * Y$$

$$64 = P - a_1 * X^3 - a_2 * Y^3$$

$$66 = P - a_1 * x^7 - a_2 * Y^7$$

$$67 = P$$

where $X = \exp(-6/L_1)$, and

$Y = \exp(-6/L_2)$

Using Loo's value of 2 hours for the time constant of traps E1 and E2, where L_2 equals 2 hours gives;

$L_1 = 23$ Hours

$L_2 = 2$ hours

$a_1 = 6.4$ mW

$a_2 = 1.6$ mW

This information along with the annealing rate at various times has been collected in Table XIII.

TABLE XIII

CELL E-10 ANNEALING CONSTANTS AND ANNEALING RATE FOR SEVERAL TIMES

Time (Hrs)	P_{max} (mW)	P (mW)	a_1 (mW)	a_2 (mW)	L_1 (Hr)	L_2 (Hr)	P´(0) (mW/Hr)	P´(6) (mW/Hr)	P´(18) (mW/Hr)
0	59								
6	62								
18	64	67	6.4	1.6	23	2	1.083	0.254	0.127
42	66								
48	67								
96	67								

VI. CONCLUSIONS AND RECOMMENDATIONS

A. CONCLUSIONS

1. Main Experiment

The GaAs solar cells were forward-biased current annealed with 0.5A/cm^2 continuous current in an ambient temperature of 90 degrees centigrade. The process recovered 28-30% of the lost power over 48 hours in solar cells E-9 and E-10. This is far short of results using thermal annealing but the energy expended was only 96 Watt-Hrs per cell. The cell temperature never exceeded 120 degrees centigrade which would not stress space array components. Cell E-10 was annealed for a total of 96 hours. In the last 48 hours annealing did not occur, but neither did cell degradation as occurred when the larger current density, 1.0A/cm^2, was used.

2. High Current Experiment

The failure when annealing at 1.0A/cm^2 was a little surprising. The cell temperature never exceeded 150 degrees centigrade, well below thermal annealing temperatures. It may be that the electronic energy transfer to the lattice plus the kT thermal energy combined to accelerate the diffusion of dopants and thereby destroying the P-N junction. A Possibility also exists that chemical reactions

occurred between the cell edges and the atmosphere, resulting in increased leakage currents across the junction.

It is interesting to note that, in both cells, the short circuit current continued to show significant improvement. The process seems to be increasing the minority carrier diffusion length, but each cell begins to fail as its electrical potential rises.

3. Application

A lot more work is required in this area, but the reward in cost savings should be substantial. Adding this type of recovery system to a current satellite would extend the life of a five year mission by almost one and one-half years and double that for a ten year mission.

Extending the mission lifetime is not always desirable as the satellite may be expected to become technologically obsolete. Using smaller solar cell arrays, then extending their useful life through annealing, would decrease the satellite size and weight; resulting in reduced material, storage and launch costs. Additionally, a satellite with less cross-sectional area would have less drag in near earth orbit, and require less fuel for station keeping.

B. RECOMMENDATIONS

The experiment was conducted using equipment on hand. As a result, several parameters of the test would not be realized in space. Follow-on experiments may include;

1. Atmosphere

Conduct the annealing in a neutral or evacuated atmosphere. This would reduce any error introduced due to chemical processes at the cell edges.

2. Light Source

Conduct the annealing with a AM0 light source illuminating the cell. This probably will change the outcome very little, but improves on the use of the incandescent light used here.

3. Front Contacts

The contacts are ohmic in nature. Passing high currents may cause localized heating and subsequent delamination, or at least an increase in the series resistance at the contacts. This area needs attention.

Other areas of interest include;

4. DLTS and Visible Spectrum Analysis

These test may help the cell manufacturer as well as the array designer in improving and implementing this process.

5. Reradiation

Subject the annealed cells to a radiation environment to observe any change in their radiation tolerance.

APPENDIX A

PRE-TRIAL USING 20Mev ELECTRON DAMAGED CELLS

Prior to performing the main experiment, several experimental trials were run. Two GaAs solar cells that had been irradiated with 20-Mev electrons for a total fluence of 1E15 el/cm^2 were used.* These cells are similar to the cell described in Table VII. One cell[ASEC-2] was current annealed using various current densities between 0.125A/cm^2 and 0.313A/cm^2 while holding the ambient temperature to 27 degrees centigrade. After 35 hours of anneal time the cell did not show any significant improvement.

ASEC-2 was then used to measure the thermal annealing at temperatures of 100 and 150 degrees centigrade. After 41 hours at 100 degrees centigrade the cell parameters exhibited a 1 to 2% improvement. The cell did show better improvement when thermally annealed at 150 degrees. The maximum power, short circuit current, and efficiency all increased 4% after five hours but never improved farther, even after 77 hours of anneal time. The open circuit voltage increased as C - exp(-K*t), but even after 77 hours

---

*The 20-Mev irradiated GaAs solar cells used in this part of the thesis were obtained from LT Donald Gold who irradiated the cells as part of the ongoing research funded by the Naval Space and Warfare Systems Command. Principal investigator for the NAVSPAWAR Solar Cell Research Project is Distinguished Professor Allen E. Fuhs. Contract Monitor is Major Michael McNulty, US Army, PDW-106.

when annealing had stopped the total improvement was only 1.2%.

ASEC-3 GaAs solar cell was used to examine the combined thermal and current annealing effect. The cell was held to 100 degrees and annealed for 4 hours using 0.125A/cm^2 forward bias current. The open circuit voltage, maximum power and efficiency all dropped significantly. This was unexpected and no explanation could be found. Increasing the anneal time started to reverse the degradation as did increasing the anneal current to 0.175A/cm^2. The ambient temperature was then raised to 150 degrees and the forward bias current adjusted to 0.125A/cm^2. All parameters gave steady improvement through 45 hours of annealing. The cell then cracked due to handling.

The following conclusions were drawn;

1) GaAs does not thermally anneal at 100 degrees centigrade and only limited annealing occurs at 150 degrees,

2) Forward bias current annealing at 0.125A/cm^2 and room temperature does not occur,

3) Annealing improves with temperature,

4) Small changes in the current density has little effect on the annealing rate, and

5) Current densities on the order of 0.125A/cm^2 are too small to affect speedy recovery.

It must be understood that these cells were irradiated with very high energy electrons, much different than that of the cells actually used in the main experiment. Therefore

one can not say with any certainly that damage mechanisms and relative numbers of any particular damage mechanism has any correlation between the two.

APPENDIX B

PRE-TRIAL USING 20Mev ELECTRON DAMAGED CELLS

It was necessary to determine at what forward bias current density the GaAs solar cells would significantly anneal. The interest at this point was not the annealing rate, but simply the final parameter values after annealing has stopped. The parameter of interest was the cell efficiency because it is essentially a function of all the other measured parameters. An improvement here implies a general improvement in the cell.

It was recognized early on that current densities below 0.3A/cm^2 with an ambient temperature of 90 degrees centigrade were ineffective.* Good results were obtained by increasing the current to 0.5A/cm^2. This was chosen as the current density for the main experiment.

---

*The annealing apparatus was placed in an oven enclosure to reduce air motion and stabilize the ambient temperature. The incandescent light caused the solar cell and the enclosure to heat above 100 degrees. It was found that leaving the oven door slightly ajar produced a fairly stable ambient temperature of 90+/-5 degrees.

TABLE B-1

2cm X 2cm GaAs SOLAR CELL E22 ANNEALED AT VARIOUS CURRENT DENSITIES WHILE HELD IN A 90 DEGREES CENTIGRADE AMBIENT ENVIRONMENT.

Time	J	V_{OC}	I_{SC}	C_{ff}	V_m	Eff	P_{max}
(Hr)	(A/cm^2)	(mV)	(mA)	(%)	(mV)	(%)	(mw)
NEW		992	119	75.0		16.4	89
1E15		903	94	79.5	760	12.5	68
5	0.025	902	91	81.0	777	12.3	67
6	0.075	904	93	80.6	774	12.5	68
12	0.150	905	92	80.5	775	12.4	67
12	0.250	906	93	80.3	777	12.5	68

TABLE B-2

2cm X 2cm GaAs SOLAR CELL E23 ANNEALED AT VARIOUS CURRENT DENSITIES WHILE HELD IN A 90 DEGREES CENTIGRADE AMBIENT ENVIRONMENT.

Time (Hr)	J (A/cm^2)	V_{OC} (mV)	I_{SC} (mA)	C_{ff} (%)	V_m (mV)	Eff (%)	P_{max} (mw)
NEW		968	119	76.2		16.1	87
1E15		896	95	79.9	772	12.5	68
5	0.050	894	92	81.3	765	12.4	67
6	0.100	897	93	81.0	776	12.5	67
12	0.200	899	93	80.6	766	12.5	67
12	0.300	898	94	79.8	767	12.5	67
12	0.500	902	98	79.9	776	13.2	71
24&	0.500	904	99	79.9	765	13.2	71
48	0.500	911	101	80.1	774	13.7	74
72	0.500	914	102	79.8	773	13.8	74
96	0.500	914	103	79.3	782	13.8	74
24	0.700	916	103	78.6	766	13.8	74
24	0.900	921	106	78.0	771	14.0	76

& The light source, and therefore the heating source, was accidentally secured at some unknown time during this part of the anneal. The light source was operational for the remainder of the test.

APPENDIX C

ANNEAL USING 1.0A/cm^2 CURRENT DENSITY

A follow-on experiment was conducted that was exactly the same as the main experiment except that a 1.0A/cm^2 current density was chosen. Solar cells E-20 and E-24 were used. The results are tabulated in Tables C-1 and C-2. In cell E-20, the open circuit voltage began to decline after seven hours of annealing. Cell E-24 experienced similar results after only one hour. In both cases the short circuit current continued to improve. More importantly, the fill factor dropped off on both cells indicating an increase in the cells' internal resistance. This current density may be an upper limit to continuous forward bias annealing without providing a cell cooling mechanism.

TABLE C-1

2cm X 2cm GaAs SOLAR CELL E-20 ANNEALED WITH CURRENT DENSITY 1.0A/cm^2 AT AN AMBIENT TEMPERATURE OF 90 DEGREES CENTIGRADE.

Time (Hr)	V_{OC} (mV)	I_{SC} (ma)	C_{ff} (%)	V_m (mV)	Eff (%)	P_{max} (mW)
0	888	103	79.2	761	13.4	72
1	891	104	79.0	752	13.5	72
2	891	103	78.9	745	13.5	73
7	892	105	77.3	742	13.4	72
24	885	110	74.1	744	13.4	72

TABLE C-2

2cm X 2cm GaAs SOLAR CELL E-24 ANNEALED WITH CURRENT DENSITY 1.0A/cm^2 AT AN AMBIENT TEMPERATURE OF 90 DEGREES CENTIGRADE.

Time (Hr)	V_{OC} (mV)	I_{SC} (ma)	C_{ff} (%)	V_m (mV)	Eff (%)	P_{max} (mW)
0	893	96	77.4	758	12.3	67
1	905	102	77.5	779	13.3	72
2	897	103	76.5	741	13.1	71
7	801	106	72.0	638	11.3	61
24	803	109	62.2	617	10.0	54

GLOSSARY

A	Amps
Au	Astronomical unit
c	Velocity of light
cm	Centimeter
DLTS	Deep Level Transient Spectroscopy
E	Energy
E_d	Atom displacement energy
E_{max}	Maximum energy
el	Electron
ev	Electron volts
exp	Exponential function
GaAs	Gallium arsenide
GaP	Gallium phosphide
hr	Hour
I	Current
I_{pmax}	Cell current at the maximum power point
I_{SC}	Cell current when short circuited
I-V	Current-Voltage (curves)
km	Kilometer
K_t	Lifetime damage coefficient
ln	Nature logarithm
M	Atom or particle mass
m	Electron mass

Mev	Million electron volt
n_a	Atom density
N_d	Volume number density
n/p	n-doped semiconductor on p-doped semiconductor substrate
OC-CVD	Organo-metallic Chemical-vapor-deposition
P	Power (electrical)
P_{max}	Maximum power
p/n	p-doped semiconductor on n-doped semiconductor substrate
Si	Silicon
t_e	Minority carrier lifetime due to electron irradiation
t_o	Minority carrier lifetime before irradiation
t_p	Minority carrier lifetime die to proton irradiation
um	Micrometer
V	Average number of displacements per primary displacement
V	Voltage
V_{OC}	Cell voltage when not passing current
V_{pmax}	Cell voltage at the maximum power point
W	Watt
@	Displacement cross section

LIST OF REFERENCES

1. Jet Propulsion Laboratory Publication 82-69, Solar Cell Radiation Handbook, 3rd ed., by H. Y. Tada, J. R. Carter, Jr., B. E. Anspaugh and R. G. Downing, 1 November 1982.

2. C. S. Yeh, S. S. Li and R. Y. Loo, A Simple Model for Calculating the Displacement Damage in Electron and Proton Irradiated AlGaAs/GaAs/InGaAs (or Ge) Multijunction Solar Cells, in Eighteenth IEEE Photovoltaic Specialists Conference, pp.657-662, 1985.

3. A. H. Kalma, R. A. Berger, C. J. Fischer and B. A. Green, "Energy and Temperature Dependence of Electron Irradiation," IEEE Transactions of Nuclear Science, NS-22, p.2277, 1975.

4. W. L. Wang and Sheng S. Li, Studies of Deep-level Defects and Recombination Parameters in One-Mev Electron and Low Energy Proton Irradiated (AlGa)As-GaAs Solar Cells, in Seventeenth IEEE Photovoltaic Specialists Conference, p.161, 1984.

5. John J. Stith and John W. Wilson, Microscopic Defect Structures and Equivalent Electron Fluence Concepts, in Eighteenth IEEE Photovoltaic Specialists Conference, pp.1716-1717, 1985.

6. Sheng S. Li, W. L. Wang, R. Y. Loo and W. P. Rahilly, Deep Level Defects and Annealing Studies in One-Mev Electrons Irradiated (AlGa)As-GaAs Solar Cells, in Sixteenth IEEE Photovoltaic Specialists Conference, pp.211-215, 1982.

7. Sheng S. Li, C. G. Choi and R. Y. Loo, Studies of Radiation-induced Defects in One-Mev Electron and Low Energy Proton Irradiated Germanium and Al(x)Ga(1-x)As P-N Junction Solar Cell, in Eighteenth IEEE Photovoltaic Specialists Conference, pp.640-645, 1985.

8. John R. Barton, William G. Dunbar and Amy C. Reiss, High Voltage Solar Array Plasma Protection Techniques, in Eighteenth IEEE Photovoltaic Specialists Conference, pp.411-417, 1985.

9. B. E. Anspaugh and R. G. Downing, Radiation Effects in Silicon and Gallium Arsenide Solar Cells using Isotropic and Normally Incident Radiation, in Seventeenth IEEE Photovoltaic Specialists Conference, pp.23-30, 1984.

10. Joseph F. Wise, Solar Power Requirements for Military Space Vehicles, in Seventeenth IEEE Photovoltaic Specialists Conference, pp.17-22, 1984.

11. S. Matsuda, M. Oloda, K. Mitsui, M. Kato, S. Hokuyo and S. Yoshida, Developement of AlGaAs/GaAs Solar Cells with Space Qualifications, in Seventeenth IEEE Photovoltaic Specialists Conference, pp.97-102, 1984.

12. D. Zemmrich, N. Mardesich, B. MacFarlane and R. Loo, Gallium Arsenide: Solar Panel Assembly Technology, in Seventeenth IEEE Photovoltaic Specialists Conference, pp.315-319, 1984.

13. R. P. Gole, John C. C. Fan, G. W. Turner and R. L. Chapman, A New High-efficiency GaAs Solar Cell Structure Using a Heterostructure Back-surface Field, in Seventeenth IEEE Photovoltaic Specialists Conference, pp.1422-1425, 1984.

14. D. W. Gold, High Energy Election Radiation Degradation of gallium Arsenide Solar Cells, Masters Thesis, Naval Postgraduate School, Monterey, California, March 1986.

15. D. V. Lang and L. C. Kimerling, "Observation of Recombination-Enhanced Defect Reactions in Semiconductors," Physical Review Letters, v. 33, n. 8, pp.489-492, 19 August 1974.

16. D. V. Lang and L. C. Kimerling, "Observation of Athermal Defect Annealing in GaP," Applied Physics Letters, v. 28, n.5, pp.248-250, 1 March 1976.

17. D. V. Lang, L. C. Kimerling, and S. Y. Leung, "Recombination-enhanced Annealing of the E1 and E2 Defect Levels in 1-Mev-electron irradiated n-GaAs," Journal of Applied Physics, v.47, n. 8, pp.3587-3591, August 1976.

18. R. Loo, R. C. Knechtli, and G. S. Kamath, Enhanced Annealing of GaAs Solar Cells Radiations Damage, in Fifteenth IEEE Photovoltaic Specialist Conference, p.1471, 1981.

19. D. Stievenard and J. C. Bourgoin, Degradation and Recovery of GaAs Solar Cells Under Electron Irradiation, in Seventeenth IEEE Photovoltaic Specialists Conference, pp.1103-1107, 1984.

20. Y. C. M. Yen, K. I. Chang and J. L. Tandon, Large Scale OM-CVD Growth of GaAs Solar Cells, in Seventeenth IEEE Photovoltaic Specialists Conference, pp.36-41, 1984.

INITIAL DISTRIBUTION LIST

		No. Copies
1.	Defense Technical Information Center Cameron Station Alexandria, VA 22304-6145	2
2.	Library, Code 0142 Naval Postgraduate School Monterey, CA 93943-5002	2
3.	Professor S. Michael Code 62Mi Naval Postgraduate School Monterey, CA 93943-5000	2
4.	Department of the Navy Commander Space and Naval Warfare Attn: Major M. L. McNulty Washington, D.C. 20363-5000	2
5.	Dr. H. B. Rigas Code 62 Naval Postgraduate school Monterey, CA 93943-5000	2
6.	Naval Space Command Code N13 Dahlgren, VA 22448	2
7.	Peter Iles Applied Solar Energy Corporation 15251 East Don Julian Rd. City of Industry, CA 91746	2
8.	Terry Trumble Energy Conversion Branch Aerospace Power Division Aero Propulsion Laboratory Wright-Patterson Air Force Base Ohio 45433	2
9.	Professor Fred R. Buskirk Code 62Bs Naval Postgraduate School Monterey, CA 93943-5000	2

10. United States Space Command 2
Attn: Technical Library
Peterson AFB, CO 80914

11. R. Francis 2
The Aerospace Corporation
P.O. Box 92957
Los Angeles, CA 90009

12. Fred Betz 2
Code 6623
Naval Research Laboratory
4555 Overlook Ave., SW
Washington, D.C. 20375

13. George Datum 2
Lockheed Missile and Space Company
P.O. Box 3504
Department 3230
BLDG 15E
Sunnyvale, CA 94088-3504

14. LT T. F. Clark 4
Defense Mobilization Systems Planning Activity
OASD/FM&P Correspondence Control Division
Room 3E759, Pentagon
Washington, DC 20301-4000

TITLE NUMBER: _____ CUSTOMER NUMBER: _____

LIBRARY: Dudley Knox Library, Naval Postgraduate School
Monterey, Ca 93943

ROSWELL BOOKBINDING
LIBRARY DIVISION
2614 NORTH 29th AVENUE
PHOENIX, ARIZONA 85009
PHONE (602) 272-9338

Binding in Everything [ ] X

	F	B	NP
CONTENTS			
INDEX			
Bind without Index			

ISSUE CONTENTS

Discard	
Bind in Place	
Gather at Front	

	IN	OUT
Advertisements		
Front Covers		
Back Covers		
1st only		
Accents		
Imprints		

Special Instructions:

THOMAS FREDRICK CLARK

94837

Thesis C4837

Buck Color	
Print Color	598.
Trim Height	Gold
Ht. Inches	
Over Thick	
For Title	
Extra Lines	
Extra Coll	
Hand Sew	
Slit	
Rules	
1st Slot No	
Vol Slot No.	
Year Slot No.	
Call # Slot	
Imp Slot No	
Type Face	
Price	
Mending	
Map Pockets	
2 Vols in 1	

ACTUAL TRIM	DATE
SPINE	JOB
BOARD DIM	LOT
CLOTH DIM	ROUTE
CLOTH BIN	SEQ NO